Thermal Science and Engineering Progress 73 (2026) 104682

Contents lists available at ScienceDirect

Thermal Science and Engineering Progress

journal homepage: www.sciencedirect.com/journal/thermal-science-and-engineering-progress

Effect of nanoparticle concentration on non-aqueous paraffin pickering emulsions in PEG400 for efficient thermal energy storage

Sebastián Sanabria, Clara Delgado-Sánchez, Adrián Tenorio-Alfonso, Antonio A. Cuadri, Francisco Javier Navarro *

Departamento de Ingeniería Química, Centro de Investigación en Tecnología de Productos y Procesos Químicos (Pro²TecS), Universidad de Huelva, Campus de "El Carmen", 21071 Huelva, Spain

ARTICLE INFO

Keywords:
Non-aqueous phase change emulsion
phase change material (PCM)
Pickering emulsion
Rheology
Thermal energy storage

ABSTRACT

The development of non-aqueous phase change material emulsions (PCMEs) for thermal energy storage holds significant potential, as it enables the extension of the operating temperature range beyond the freezing and boiling points of water. Nevertheless, achieving stable and processable formulations remains a significant challenge. In this regard, this research presents the formulation and characterization of anhydrous Pickering emulsions, in which a selected paraffin (melting point 58–60 °C) serves both as the dispersed phase and as the phase change material (PCM), while polyethylene glycol (PEG 400) constitutes the continuous phase. The emulsions were stabilized with hydrophobized pyrogenic silica nanoparticles, and the influence of nanoparticles concentration on emulsion morphology, rheology, and thermal properties was evaluated. Characterization techniques included optical microscopy, steady-state flow measurements, oscillatory tests, and modulated differential scanning calorimetry (MDSC). The results demonstrate that the nanoparticles successfully stabilize the emulsions and enhance their rheological properties, which is attributed to internal structuring mechanisms. Additionally, only minimal supercooling was detected in the samples. Overall, the formulated emulsions exhibit tuneable properties and offer a promising platform for the design of PCME systems capable of stable operation at elevated temperatures, including applications in solar–thermal energy capture.

1. Introduction

The increasing global demand for energy, driven by population growth and technological advancements based on fossil fuels, has raised concerns about climate change and greenhouse gas emissions [1]. To ensure a sustainable future, it is important to promote the use of renewable energy sources, such as solar and wind power, which can be an effective way to address the energy crisis without causing further harm to the environment. However, renewable energy sources face a significant challenge in achieving a progressive reduction and substitution of fossil-based energy due to a mismatch between energy generation and consumption. Thus, to achieve a progressive optimization of renewable energy, excess energy from these fluctuating sources must be stored to bridge the gap between energy gathering and demand. Thermal energy storage (TES) is one of the most efficient means to achieve it [2].

TES refers to the temporary accumulation of thermal energy in the form of heat or cold for later use. TES systems are characterised by high efficiency, short charging and discharging cycles, economic efficacy, and safety [3,4]. Although most practical applications typically make use of sensible heat storage systems, latent heat storage offers significantly higher storage density, smaller volumes and operational advantages, with minimal temperature variation during the charging and discharging processes. It has proven to be an efficient method of storing thermal energy [5,6].

Therefore, the use of phase change materials (PCMs) for latent heat storage is highly relevant due to their high energy density and ability to store or release a significant amount of heat within a constant temperature range during phase transition, typically between liquid and solid states. This makes them a promising option for various applications, including solar thermal systems, building insulation and thermoregulation, food storage, and transportation [7,8]. Among TES systems based on PCM, phase change material emulsions (PCMEs) represent a viable, relatively low-cost and straightforward formulation of advanced heat

* Corresponding author.
E-mail addresses: clara.delgado@diq.uhu.es (C. Delgado-Sánchez), frando@uhu.es (F.J. Navarro).

https://doi.org/10.1016/j.tsep.2026.104682
Received 23 December 2025; Received in revised form 25 March 2026; Accepted 30 March 2026
Available online 1 April 2026

transfer fluids [9] that enables not only energy storage but also its transport from the production site to the end-use location. These PCMEs consist of PCM dispersed in the form of droplets in an immiscible carrier fluid, which acts as the continuous phase, stabilized by an emulsifying agent [10]. Then, this alternative has a high thermal storage capacity derived from the combined sensible and latent thermal capacities of the carrier fluid and PCM. Therefore, PCMEs endow heat transfer fluids with new functional properties, such as enhanced fluidity, pumpability, and efficient transport of the thermal energy absorbed or released during phase-change transitions [9,11]. Nonetheless, achieving long-term stability and mitigating supercooling remain challenging aspects in PCME formulation for the effective implementation [12].

In practice, the development of PCMEs have mostly been developed using aqueous paraffin-based systems, which remain the most extensively studied to date [9,13]. Representative examples include tetradecane or n-octadecane in water emulsions stabilized with a mixture of non-ionic surfactants such as Tween 60 and Span 60 [14] or Tween 20 and 1,3-butanediol [15], respectively. Emulsions containing n-hexadecane stabilized with organic surfactants such as Span 80 [15] and Tween80 [16] have also been reported. Beyond to paraffin-based systems, fatty acid–based emulsions have also received considerable attention. These include formulations incorporating stearic acid, capric acid, lauric acid, myristic acid, and palmitic acid, as well as eutectic mixtures of these components. Such systems are typically stabilized using combinations of ionic surfactants (e.g. sodium dodecyl sulfate, SDS) and non-ionic surfactants (e.g. Span 20) [17]. As well as other organic PCMs, including long-chain alcohols (1-hexadecanol) [18] and fatty acid esters (Crodatherm 53 and Crodatherm 47) [19] have also been emulsified using tailored surfactant blends (ionic or non-ionic) depending on the formulation goals.

Beyond the choice of PCM and surfactant, the immiscibility between the PCM and the carrier fluid largely determines the emulsion development. Depending on PCM solubility, PCMEs can be formulated as PCM-in-water (O/W) when water is the continuous phase, or PCM-in-oil (O/O) for water-free systems [11]. In addition, the preparation method plays a key role in defining the emulsion type. Emulsions may be produced using high-energy or low-energy techniques depending on the application and desired properties [20]. High-energy methods rely on mechanical shear to break large droplets into smaller ones (5–100 μm), with disruptive forces generated by devices such as rotor–stator systems, ultrasonicators, high-pressure homogenizers, microfluidizers, or membranes. In contrast, low-energy methods exploit the physicochemical properties of surfactants rather than external energy input. These approaches, including phase inversion temperature (PIT) and emulsion inversion point (EIP), enable a controlled transition between oil-in-water and water-in-oil systems, often producing uniform, and stable emulsions [9,11].

In this context, numerous studies have investigated both conventional and emerging applications of aqueous PCMEs for heating and cooling purposes. Notable examples include their use in photovoltaic heat dissipation [21], cold storage for building radiant cooling systems [22], battery thermal management [23], heat exchangers [24], and heat dissipation in temperature-sensitive electronic components of high-voltage direct current converters operating at 50 °C [19].

Although the practical applications of energy storage with PCMEs are a relatively recent development requiring further research, existing studies have only presented aqueous-based emulsions where paraffins are stabilised by surfactants [9,25,26]. Thus, studying alternative formulations may offer additional advantages in terms of versatility and efficiency [11,27]. For instance, oil-in-oil (o/o) emulsions, characterized by the presence of two immiscible oil phases, represent a notable improvement over the traditional oil–water emulsions, allowing to expand the in-service temperature range [28,29]. These emulsions have demonstrated resilience and stability against heating–cooling cycles while preserving their properties and heat storage capacity[30]. Moreover, these formulations could be suitable for applications where water is incompatible or where higher or lower operating temperatures than the freezing and boiling points of water are required [31,32].

In addition, Pickering emulsions have attracted increasing attention as an alternative stabilisation method to traditional surfactants for thermal storage applications, due to their notable resistance to coalescence, high thermochemical stability, operational reliability and environmentally sustainable profile [33–35]. This approach involves using solid particles to stabilise immiscible phases by forming a dense layer of particles at the interface. This layer acts as a steric barrier, preventing PCM droplet coalescence and providing improved stability to the emulsion. In this regard, the stabilization mechanism in Pickering emulsions relies on the partial wetting behaviour of the solid particle surface by both liquid phases [36–38]. The adsorption of solid particles at liquid–liquid interfaces with very large desorption energies makes Pickering emulsions typically exhibit higher stability than surfactant-stabilized emulsions, as the particles form a robust and often irreversible interfacial barrier [39]. In contrast, molecular surfactants used in phase change material emulsions (PCMEs) may undergo thermal degradation or experience reduced interfacial activity at elevated temperatures [40,41], which limits their performance in medium and high temperature thermal energy storage systems. Various applications of Pickering emulsions have been widely studied [36–38], but only recent researches have focused on formulating this type of emulsion for latent heat storage, using mainly oil-in-water emulsion stabilized by nanomaterials such as oxides [42,43], polysaccharides [34,44] and polymers [45,46].

Among various PCMs, paraffin waxes exhibit several superior properties compared to other PCMs, including low cost, high thermal storage density, chemical inertness, low vapour pressure, non-segregation, non-corrosiveness, and resistance to subcooling. These characteristics make them attractive for a range of applications, such as solar drying systems, solar energy collectors, electronic cooling, and building materials. However, their inherently low thermal conductivity remains a significant limitation in practical implementation [47–49].

Pickering oil-in-oil (O/O) phase-change emulsions address the intrinsic volatility, chemical incompatibility, and temperature constraints that may limit the performance of conventional water-based PCMEs. By employing solid particles to stabilize the interface between two immiscible organic liquids, instead of traditional surfactants, these systems exhibit enhanced thermal stability, tuneable rheological properties, and a pronounced resistance to coalescence [50]. The combination of Pickering stabilization with fully non-aqueous continuous phases affords robust operation under high-temperature and water-sensitive conditions, thereby positioning O/O PCMEs as a distinctly innovative platform for advanced thermal-energy-storage applications and related technologies.

The main objective of this study was to develop and characterise stable non-conventional oily PCMEs to investigate their potential as a thermal energy storage system. Specifically, a selected paraffin wax (melting point of 58–60 °C) was used as PCM, and a polyethylene glycol (PEG 400) was employed as polar heat transfer fluid which remains liquid and stable across the PCM phase transition temperature range. Finally, surface-modified hydrophobic pyrogenic silica nanoparticles were selected as the Pickering emulsion stabiliser, with a portion of the highly polar Si–OH groups on their surface chemically replaced by non-polar silane groups. This modification conferred partial hydrophobicity, enhancing the affinity between the two immiscible phases and thereby improving emulsion stability [51,52]. This work also seeks to generate fundamental knowledge that can guide the future development of Pickering emulsions engineered to function at temperatures exceeding 100 °C, a type of system that remains unexplored to date [9]. In pursuit of a deeper understanding of this non-conventional system and the effect of nanoparticles on it, the thermophysical and rheological properties of the emulsions were thoroughly analysed. Initially, changes in the surface tension of the continuous phase were measured. Next, the emulsion microstructure was identified and examined. Then, viscous and

viscoelastic behaviour was studied and, finally, the thermal properties were measured and its potential use as a thermal energy storage system was discussed.

2. Experimental

2.1. Materials

This study employed a polyethylene glycol with an average molecular mass 400 g/mol (PEG 400, $H(OCH_2CH_2)_nOH$), as the continuous phase. PEG presents of a linear chain structure composed of repeating ethylene oxide groups possessing a hydroxyl group (–OH) at both ends, where the presence of oxygen atoms provides some hydrophilic character and polarity[53,54]. Granulated paraffin (pure, pharma grade, melting point 58-60 °C) was used as the dispersed phase of phase change material (PCM). PEG 400 was obtained from Merck Life Science S.L (Spain), and the paraffin from PANREAC QUIMICA S.L.U. (Spain). Trimethoxyoctylsilane-modified pyrogenic silica nanoparticles (Aerosil R-805, BET 125–175 $m^2 \cdot g^{-1}$) were employed as the emulsion stabilizer. Their surface functionalization imparts partial hydrophobicity and generates an intermediate wettability that is optimal for interfacial adsorption and emulsion formation, as described in the previous section. Aerosil R-805 was purchased from Evonik Operations GmbH, Germany.

2.2. Preparation of samples

2.2.1. Anhydrous pickering PCMEs

Pickering PCMEs were prepared by mixing molten paraffin with PEG 400, at 80 °C, using Aerosil R-805 as emulsifier. Fig. 1 shows a likely structural formulation of the nanoparticle and its possible stabilization mechanism in the present emulsion. To investigate, first the minimal amount of nanoparticles required to form the emulsions and then the impact of nanoparticle concentration on the properties of the PCMEs, samples with varying weight concentrations of stabilizer (0.10, 0.25, 0.50, 1.00, and 3.00 wt%) were prepared, while maintaining a constant ratio of dispersed phase to continuous phase (1:4). These concentrations were selected to span a representative operational window that covers the transition from insufficient interfacial coverage to particle-rich regimes.

As an example, to prepare an emulsion at a 1.00 wt% of nanoparticles concentration, 0.31 g of Aerosil R-805 was added to 24 g of PEG 400 with gentle stirring at room temperature. Then, 6 g of paraffin was added, and the mixture was heated in an oven at 80 °C for one hour. Subsequently, the dispersion was performed with an Ultra-Turrax T25 homogenizer (IKA-Werke GmbH & Co. KG, Germany) at 80 °C and 20000 rpm for 5 min.

Each sample was designated as 'PCME' to indicate a phase change material emulsion, followed by the corresponding nanoparticle concentration in weight percentage of Aerosil R805 nanoparticles. For instance, the sample labelled as PCME-1.00%, whose preparation has been described in the previous paragraph, contains 1.00 wt% of nanoparticles.

2.2.2. Binary blends

Binary blends of each phase with different nanoparticle concentrations were also prepared. Aerosil R-805 was incorporated into pure molten paraffin or PEG 400, at 80 °C, and the mix was homogenized utilizing an Ultra-Turrax T25 at 20000 rpm for 5 min. Each sample was designated as 'PG' for PEG or 'PF' for paraffin, and subsequently by 'NP' for nanoparticles along with their specific concentration. For example, PG-NP-1.00% corresponds to a binary bend of polyethylene glycol with 1.00% of Aerosil nanoparticles.

2.3. Material characterization

2.3.1. Surface tension characterization

Modifications in the surface tension of the continuous phase with nanoparticle concentration, PEG 400, were measured using a Sigma 703D force tensiometer (Biolin Scientific, Finland) with a Wilhelmy plate (resolution of ± 0.01 mN/m) and following the procedure

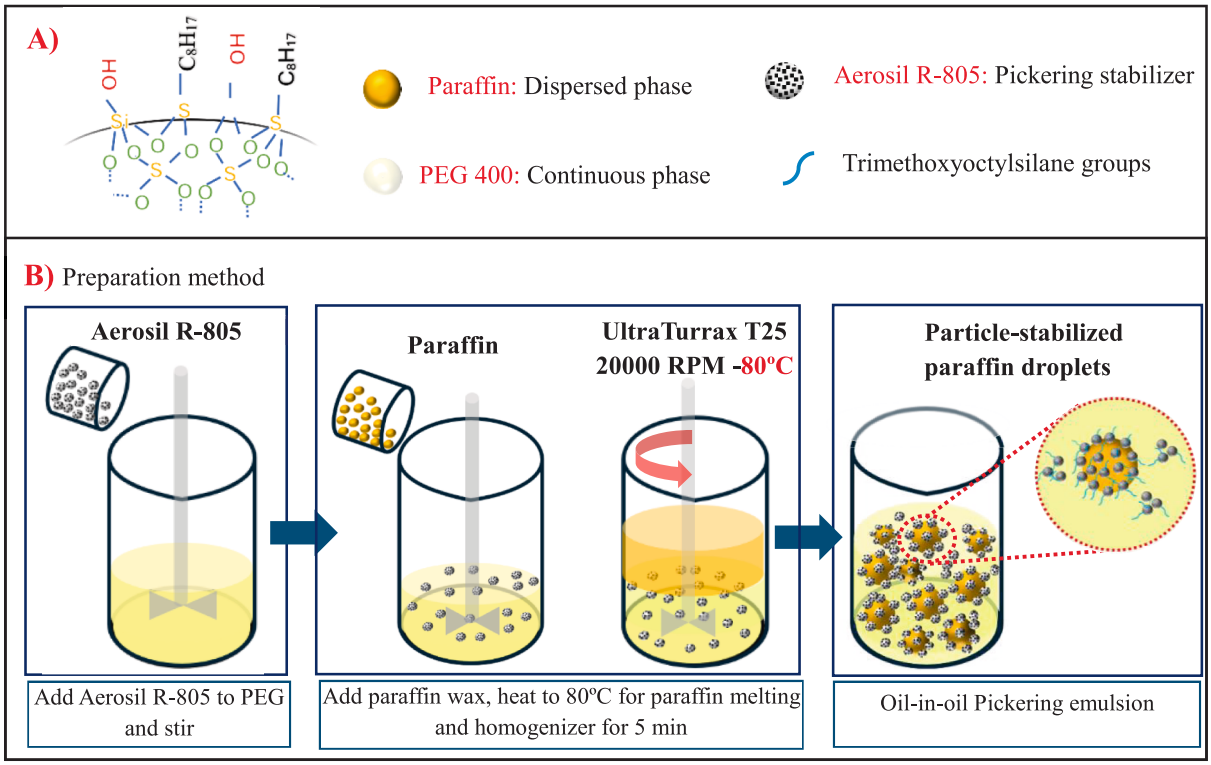

Fig. 1. A) Aerosil R-805 structure and B) Preparation method and possible stabilization mechanism.

described in literature[55]. A platinum measuring plate was suspended from a balance, and the glass sample container was placed on the sample stage. The tests were conducted at room temperature (24 °C), and each sample was measured, at least, four times.

2.3.2. Optical microscopy

The size and morphology of the dispersed paraffin droplets in emulsions were characterized using an optical microscope (Olympus BX51, Japan) equipped with an LTS-350 Heating-Freezing Stage, controlled by a Linkam TP94 system (Linkam Scientific Instruments, UK). This setup allowed precise thermal regulation during imaging.

Samples were prepared by placing a small droplet of the emulsion onto a standard glass slide, which was maintained at 80 °C to ensure the complete melting of the dispersed phase. Optical micrographs were acquired at three key stages of the thermal cycle: (i) at 80 °C, when the paraffin was fully in its molten state; (ii) after cooling to 25 °C, when crystallization had occurred; and (iii) upon reheating to 80 °C to assess any structural modifications. In addition to conventional bright-field microscopy, polarized light imaging was performed at 25 °C under crossed polarizers to provide further insight into the crystalline structure of the paraffin phase. Images were acquired from two independent samples, and for each physical state three micrographs per sample were recorded.

Droplet size distributions were determined by measuring over 500 individual droplets per sample using ImageJ software. The average droplet diameter was expressed as the Sauter mean diameter ($d_{3,2}$), a parameter that accounts for the surface-to-volume ratio of the droplets. Furthermore, ImageJ was also employed to calculate the average circularity (C), which quantifies the deviation of droplet shape from an ideal circle. Notably, samples with the highest concentration of nanoparticles (PCME-3.00%) exhibited an overly compact structure with overlapping droplets, rendering direct optical measurements unfeasible. To mitigate this limitation, a controlled dilution step was performed, wherein 1 mL of the emulsion was dispersed into 10 mL of the continuous phase to isolate smaller droplet assemblies for analysis.

Sauter mean diameters and circularity values were systematically determined for all samples at each stage of the thermal cycle to evaluate the influence of phase transitions on droplet morphology.

2.3.3. Rheological characterization

The rheological behaviour was analysed using a controlled-stress Physica MCR 501 rheometer (Anton Paar GmbH, Graz, Austria), equipped with a plate-plate geometry (50 mm diameter, 0.5 mm gap) featuring a torque resolution of 0.1 nN·m and a normal force resolution of 0.002 N. Temperature control was achieved through double Peltier elements. Isothermal steady-state flow viscous tests were conducted on the binary mixtures, PCME samples and raw materials, at 25 °C and 80 °C, under shear-stress-controlled conditions, spanning shear rates from 10^{-4} to 10^{3} s^{-1}. The linear viscoelastic behaviour was further examined using small-amplitude oscillatory shear frequency sweep tests within the linear viscoelastic range, previously established by amplitude sweep tests at constant temperature. These tests were carried out at 25 °C and 80 °C, covering a frequency range from 0.01 to 100 rad/s. Each rheological test was performed in triplicate to ensure reproducibility and to account for experimental variability.

2.3.4. Modulated differential scanning calorimetry (MDSC)

Phase change transitions of PCMEs, as well as those of binary mixtures of paraffin and nanoparticles (PF-NP-1.00%) and raw materials were analysed using a Q-250 Differential Scanning Calorimeter (TA Instruments, USA) which features a baseline stability of $\leq$ 10 μW according to manufacturer specifications. Samples weighing 10–20 mg were hermetically sealed in aluminium crucibles. A constant N_2 flow of 50 mL/min was maintained to create an inert atmosphere, minimizing oxidative effects.

Thermal measurements were conducted using a modulation period of 60 s, with a temperature oscillation amplitude of ± 0.3 °C. The heating and cooling rates were set at 2 °C/min over a temperature range of 0 °C to 100 °C, ensuring the complete melting and solidification of the dispersed phase. The experimental protocol consisted of an initial heating ramp from room temperature to the upper limit to eliminate any thermal history, followed by a cooling cycle to the lowest temperature and a subsequent second heating ramp. The melting and crystallization peak temperatures (T_m^{Peak}, T_c^{Peak}), onset temperatures (T_c^{Onset}, T_m^{Onset}), along with the corresponding total entalphies (ΔH_m, ΔH_c) and normalised enthalpies (by gram of PCM, $\Delta H_{m\,(n)}$, $\Delta H_{c\,(n)}$,) were determined. To ensure reproducibility and consistency, all calorimetry measurements were carried out in at least two independent repetitions.

2.4. Thermal conductivity

The thermal conductivity of the samples was determined in triplicate using the Transient Hot-Bridge (THB) technique, employing a THB-100 instrument (Linseis GmbH, Germany) equipped with a THB6K metal sensor. The uncertainty of the THB-100 instrument is estimated to be within ± 3%, according to manufacturer specifications. The temperature was controlled by a drying Oven SLW 53 Smart PRO (POL-EKO, Poland). Thirty millilitres of each sample were transferred into the measurement vessel, ensuring full and uniform contact with the sensor, and allowed to equilibrate for at least 2 h prior to analysis.

3. Results and discussion

3.1. Interfacial properties of emulsions

The interfacial properties of emulsions play a crucial role in determining their stability and performance across various applications, as they provide key insights into the interactions between the stabilizer and the continuous phase, as well as into formulation, stabilization mechanisms, and eventual breakdown.

Fig. 2 presents the surface tension (σ) of pure PEG 400 and silica nanoparticle suspensions in PEG 400 (PG-NP-%). The measured value for PEG 400 was 40.58 mN/m, which is consistent with previously reported data in the literature [56]. The addition of 0.25 wt% nanoparticles led to a slight reduction in surface tension, which decreased gradually with increasing nanoparticle concentration and showed a more pronounced drop above 1 wt% [57,58].

The slight decrease in surface tension observed upon nanoparticle

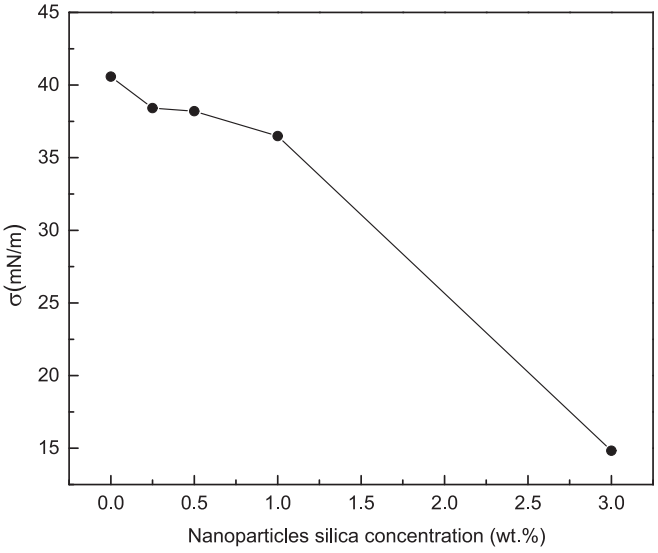

Fig. 2. Surface tension measurements(σ) of binary mixtures of PEG 400 and nanoparticles at different concentrations.

addition can be attributed to the adsorption of hydrophobized silica nanoparticles at the PEG–air interface, which modifies the interfacial free energy of the system. According to the manufacturer, the nanoparticles exhibit intermediate polarity, which provides them with partial affinity for PEG and enables their accumulation at the interface [59]. Although their ability to lower surface tension is limited compared with molecular surfactants, such interfacial adsorption is energetically favourable and accounts for the observed trend [60]. As the nanoparticle concentration increases, the greater number of particles available to reach the interface increases the probability of adsorption. As a result, the decrease in surface tension becomes more noticeable, although it remains moderate. This behaviour indicates that the nanoparticles modify interfacial conditions in a way that later contributes to emulsion stabilization. However, additional stabilization mechanisms, such as steric hindrance and viscous-related effects, are likely to play a more significant role in the stabilization of Pickering emulsions[61].

3.2. Morphological characterization of emulsions

Following the surface tension analysis, a detailed examination of PCMEs morphology is essential to understand the influence of stabilizer concentration on key parameters such as droplet structure, size, shape and distribution. Moreover, this analysis provides valuable insights into the emulsions' impact on thermal and kinetic stability, as well as on rheological properties, including viscosity and microstructural organization[62], that will be comprehensively analysed in the following sections.

Optical micrographs of the PCMEs were captured at 80 °C, where the paraffin remains in its molten state, under constant paraffin content and varying nanoparticle concentrations. This analysis aimed to evaluate the effect of the stabilizer concentration on droplet size and morphology, as shown in Fig. 3 (A1-E1). The Sauter mean diameter ($d_{3,2}$) and droplet circularity (C), as defined in Equations (1) and (2), respectively, are presented for each emulsion sample in Table 1.

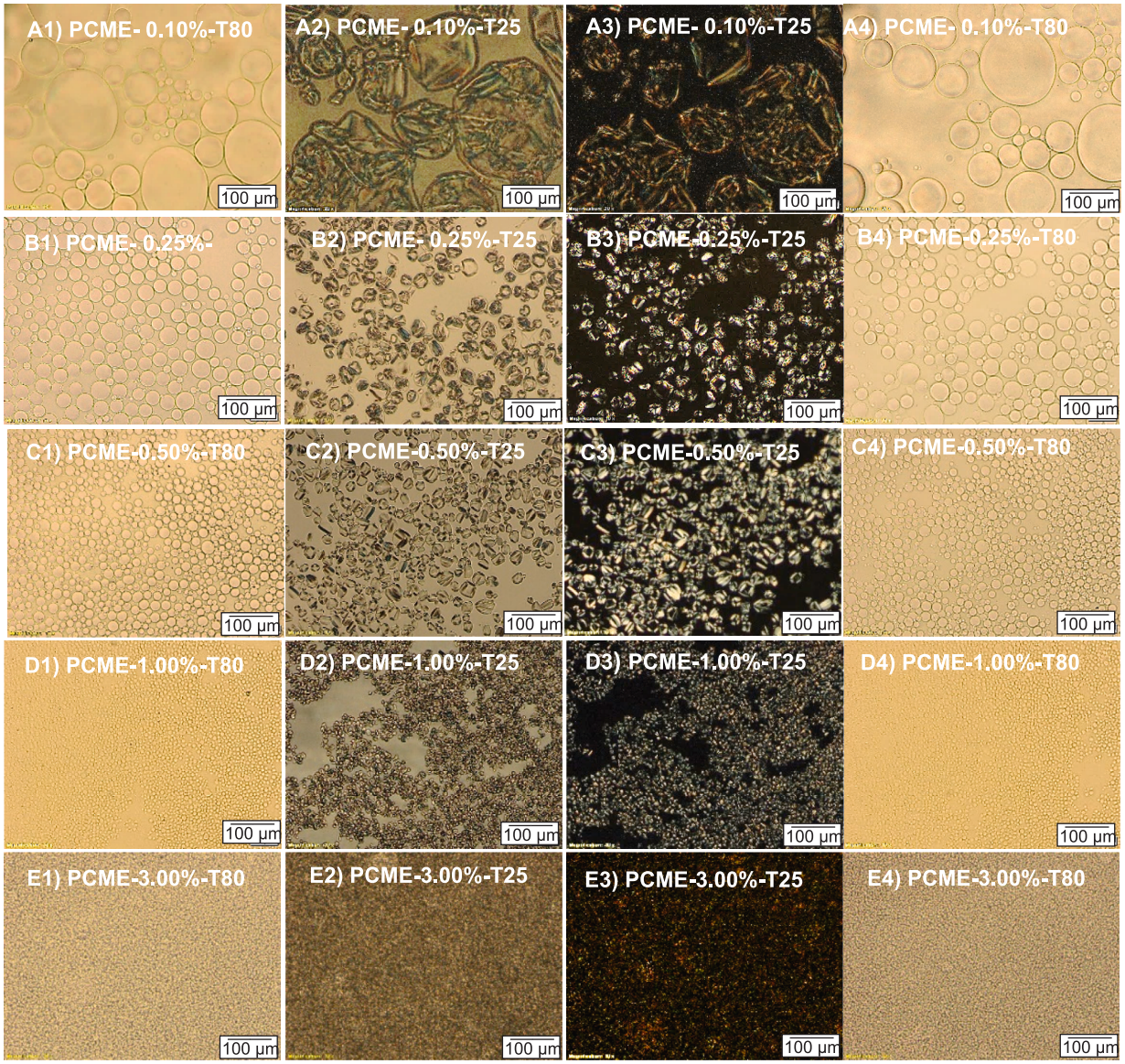

Fig. 3. Optical micrographs of emulsion samples during a cooling-reheating process, captured under unpolarized light (column 1, 2 and 4) and cross-polarized light (column 3). Images correspond to the following temperatures: 1) 80 °C, 2) 25 °C, 3) 25 °C, 4) 80 °C and at different nanoparticle concentrations: A) 0.10 wt%, B) 0.25 wt%, C) 0.50 wt%, D) 1.00 wt%, E) 3.00 wt%.

Table 1
Mean particle size ($d_{3,2}$) and circularity (C) of paraffin droplets at different stages of the cooling-reheating cycle (80 °C-25 °C-80 °C).

Sample	Fresh (80 °C)		Cooled (25 °C)		Reheated (80 °C)	
	$d_{3,2}$ (μm)	C	$d_{3,2}$ (μm)	C	$d_{3,2}$ (μm)	C
PCME-0.01%	128.14	0.987	153.42	0.726	155.12	0.985
PCME-0.25%	30.57	0.999	33.2	0.823	29.53	0.999
PCME-0.50%	17.66	0.999	17.1	0.836	15.27	0.999
PCME-1.00%	7.20	0.997	7.01	0.897	7.10	0.998
PCME-3.00%	3.09	0.998	3.12	0.912	3.07	0.998

$$d_{3,2} = \frac{\sum_i n_i \cdot d_i^3}{\sum_i n_i \cdot d_i^2} \quad (1)$$

$$C = 2\pi \frac{Area}{Perimeter^2} \quad (2)$$

Microscopy images taken at 80 °C revealed spherical paraffin droplets uniformly distributed through the continuous PEG phase, except for the PCME-3.00% sample, which exhibited a densely packed morphology. This observation suggests that, as the concentration of Pickering particles increases, the emulsion structure tends to be arranged in a network-like pattern.

As shown in Table 1, the average droplet size decreased by approximately two orders of magnitude as the nanoparticle concentration increased from 0.10 to 3.00 wt%, a fact that suggests an enhancement in the emulsion's stability, as smaller droplets are less prone to destabilization [63]. This result demonstrates a clear correlation between silica nanoparticle content and droplet size, whereby an increased availability of nanoparticles at the interface enables the stabilization of progressively smaller droplets [64].

These morphological trends can be attributed to the way hydrophobized silica nanoparticles interact with the oil–oil interface during emulsification. As the nanoparticle concentration increases, a larger number of particles becomes available to irreversibly adsorb at the molten paraffin/PEG interface. This higher particle availability, together with the progressive reduction in interfacial tension, facilitates the stabilization of a larger interfacial area [63,65–67]. However, according to Table 1, the observed decrease of droplet size approaches a constant minimum value with nanoparticle concentration, indicating a limit in the attainable diameter which appears to contradict the above. Nevertheless, this limitation likely reflects a reduction in emulsification efficiency at the highest emulsifier contents, which would otherwise allow the formation of smaller droplets. This could potentially be improved by increasing the mixing energy through enhanced mechanical or ultrasonic processing, thereby facilitating the stabilisation of larger interfacial areas[68]. In addition, this outcome suggests that silica nanoparticles are not only located at the interface but also present in excess beyond it, promoting crowding and particle–particle interactions that lead to the network-like structures observed at high concentrations and thus affecting the bulk properties of the emulsion.

Additionally, the observed decrease in droplet size (Fig. 2) may be partially attributed to the reduction in interfacial tension, which facilitates droplet breakup during the emulsification process and improves their adsorption, leading to a stronger interfacial layer[69]. It is important to note that, at the lowest nanoparticle concentration (PCME-0.01%), the emulsion underwent static destabilization, at 80 °C, in less than one hour and, as a result, no further testing was performed on this sample. This finding highlights the minimal amount of hydrophobised fumed silica required to successfully stabilize an emulsion containing 20 wt% of disperse phase[51].

To examine changes in emulsion morphology resulting from solidification of the disperse phase, cross-polarized light was also used to visualize the PCM crystallisation at 25 °C, a temperature well below the major crystallization point (Fig. 3, **A3-E3**). In optical micrographs, paraffin crystals appear as bright regions with rough texture, polyhedral geometry and a uniform distribution. The colours observed in the paraffin crystal under cross-polarized light are associated with birefringence, a phenomenon in which a light beam passes through a crystalline structure, splitting into two rays with different propagation velocities[70].

Thus, the previously mentioned instability at the lowest nanoparticle content is consistent with the observed increase in droplet size during the cooling-heating cycle, as reported in Fig. 3 **(A)** and Table 1. In this formulation, the nanoparticle layer formed at the interface is not dense enough to provide a suitable stabilisation. As a result, crystal growth occurs during the liquid-to-solid phase transition of paraffin, causing crystals to extend from the interface and connect adjacent droplets.

In contrast, minor changes in the average droplet size of the emulsions were detected during crystallization as nanoparticle content increased. The polyhedral geometry of the dispersed phase at 25 °C clearly indicates a deviation from the circular shape form during the phase change, as quantified by a moderate decrease in circularity (Table 1, Fig. 3 **(A2-E2)**). The formation of non-spherical paraffin crystals during the cooling of paraffin-based emulsions has also been reported by other authors for water-based emulsions[68,71–73] and associated with two mechanisms. The first one attributes these shape transformations to the development of interfacial multilayers of self-assembled molecules in rotator phases, structured by a solid stabilizer area. And, the second mechanism suggests that an ultralow interfacial tension in the emulsion upon cooling enables droplet deformation with minimal energy cost[74,75]. Regardless of the mechanism, non-spherical rough crystals within emulsions can cause significant variations in the thermomechanical properties with respect to those containing spherical liquid droplets[68,76].

Partial coalescence is one of the possible phenomena which can affect the properties of emulsions during paraffin crystallization [77–79]. As previously commented, this effect becomes more pronounced during droplet crystallization, as larger rough crystals at the interface protrude into the continuous phase, penetrating adjacent droplets and connecting their surfaces[38,64,80]. This phenomenon is undesirable in PCMEs, as it can lead to phase separation, particularly after droplets remelting[77]. However, in the PCME presented in this research work, optical images revealed well-dispersed droplets, showing no signs of merging, at nanoparticle concentration greater than 0.1 wt% even though crystallization seems to promote the formation of aggregates at the highest concentrations (Fig. 3**)**. Moreover, after emulsion reheating to 80 °C, remelted droplets regained their original distribution, droplet sizes and spherical shapes (**C > 0.999**), as it is illustrated in Fig. 3(A4-E4) and Table 1. This supports the idea that solid nanoparticles can prevent or slow down coalescence by forming a physical barrier around the droplets, even at low concentrations[38,64,81,82]. Therefore, increasing the nanoparticle content is likely to promote greater adsorption of particles at the interface, leading to the formation of a densely packed layer that prevents coalescence and minimises deviations from spherical morphology, thereby enhancing droplet circularity.

As a result, the morphological observations demonstrate that the oil-in-oil Pickering PCMEs were successfully stabilised, exhibiting a uniform droplet distribution and stability across different nanoparticle concentrations. Furthermore, these findings suggest good thermal stability after cooling and reheating cycles, providing a solid foundation for further analysis. Subsequently, rheological and thermal tests were conducted to gain a deeper understanding of the emulsions' characteristics.

3.3. *Rheological characterization of PCMEs*

It is well established that both rheological behaviour and stability of PCMEs are governed by factors such as emulsion structure, droplet size, stabilizer concentration, and temperature[83]. A proper balance among these properties is essential for ensuring both emulsion stability and

processability, particularly in applications where viscosity control is critical for minimizing pump energy consumption. To better understand these aspects, the following subsections analyse the viscous flow and viscoelastic properties of the systems.

3.3.1. *Viscous flow behaviour of binary mixtures*

The reported evolution of droplet diameter with increasing stabiliser concentration suggests that nanosilica particles are present in excess and may be dispersed within either phase. Then, for an effective Pickering stabilization, where particles are adsorbed at the interface, the selected nanosilica must exhibit partial compatibility with both phases. This dual affinity would affect the rheological behaviour of individual components and, ultimately, that of the emulsion as a whole.

Thus, to investigate this effect, flow experiments were firstly conducted on the two binary mixtures: nanoparticles-PEG 400 and nanoparticles-paraffin, at 80 °C. These tests aimed to investigate potential changes in rheological behaviour induced by varying nanoparticles concentrations (Fig. 4).

Fig. 4 shows that while both pristine PEG 400 and paraffin exhibited a Newtonian response with the lowest viscosities at 80 °C, the addition of nanoparticles significantly altered their flow behaviour. A pronounced shear-thinning behaviour appears for both sets of binary mixtures, starting at nanoparticle concentrations of 0.5 wt% for PEG and 1.0 wt% for paraffin, followed by an infinite-shear-rate viscosity plateau. This resulted in viscosity increases of more than five orders of magnitude, at low shear rates.

This outcome highlights the compatibility of hydrophobic silica nanoparticles with both phases, acting as thickening agents, a role that became increasingly pronounced at higher concentrations. The addition and subsequent homogenization of silica nanoparticles yielded a notable structuring effect within the raw materials matrix, pointing out its dispersibility at a nanoscale level in both phases. Interestingly, even though molten paraffin wax exhibited lower viscosity than PEG 400, at 80 °C, its binary blends with the modified nanosilica reversed this trend displaying slightly higher viscosity values. This result reflects that, although the nanomodifier is highly compatible with both phases, it demonstrates a slightly greater ability to influence the flow behaviour of the paraffin phase. This is generally attributed to the chemical modification of Aerosil R805 particles, which strongly reduces their polarity. Their polarity was initially hydrophilic and polar due to the presence of silanol groups and, after surface treatment, the silica surface becomes approximately

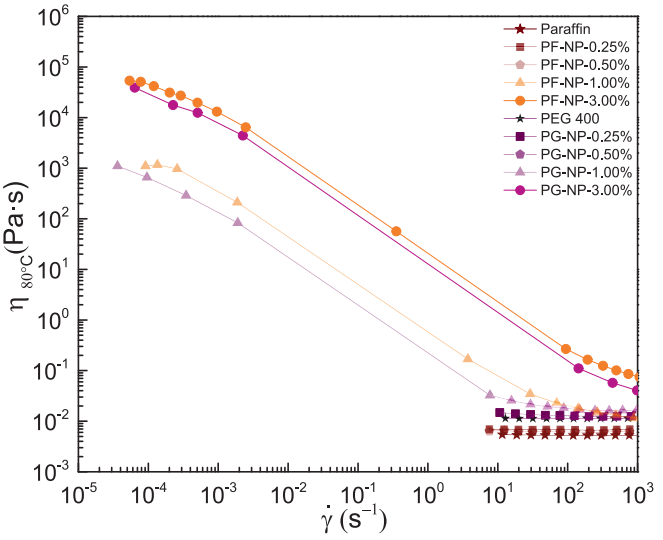

Fig. 4. Flow curves at 80 °C for pure PEG 400 and paraffin, and their corresponding binary blends with nanoparticles at varying concentrations. Samples are labelled as PG-NP-x% for PEG 400 and PF-NP-x% for paraffin, where x denotes the nanoparticle concentration (wt.%).

48% covered with non-polar octyl groups[84]. As a result, the supplier classifies this nanosilica as non-polar and highly hydrophobic, making it more compatible with the paraffin wax phase (Hildebrand solubility parameter ~ 16 $MPa^{1/2}$ [85]) compared to the PEG400 (Hildebrand solubility parameter ~ 23 $MPa^{1/2}$) which is moderately polar. Nevertheless, the flow curves also suggest an amphiphilic character of Aerosil® R 805 likely due to the partial surface coverage with hydrophobic groups, leaving a significant portion of hydrophilic sites still uncovered, which is consistent with the interfacial activity reported by the surface tension measurements.

The pronounced viscosity increases and shear-thinning behaviour observed in both PEG- and paraffin-based nanoparticle mixtures can be rationalized by the progressive formation of particle networks within each medium through two potential mechanisms. On the one hand, hydrophilic media such as PEG 400 are known to minimize interface contact with hydrophobic silica particles. This behaviour likely drives the silica particles into closer proximity, limiting the accessibility of residual silanol groups on the treated silica for interaction with polar groups in PEG. As a result, this restriction may enhance particle–particle interactions, facilitating network formation and contributing to the increase in viscosity[51,86,87]. And, on the other hand, a bridging mechanism may arise from the attractive physical interactions between the octyl chains on the surface of the silica nanoparticles, promoting the formation of agglomerates[51,52]. These structures restrict molecular mobility at low shear rates and account for the large zero-shear viscosity increase. Under applied shear, partial network disruption leads to the observed shear-thinning response and the eventual approach to an infinite-shear viscosity plateau. Moreover, as shown in Fig. 4, a minimum nanoparticle concentration, specifically above 0.25%, is required to induce noticeable changes in the rheological behaviour. This progressive structuration explains the existence of a critical concentration above which structural connectivity becomes continuous and rheological contributions from particle structuring dominate over the intrinsic viscosity of the fluid phases. At concentrations exceeding this threshold, the close proximity of silica nanoparticles enhances attractive interactions between them[51] and promote the development of gel-like structures[87].

Thus, intermediate-polarity nanoparticles structuring appears to be independent of the medium's polarity, as it occurs in both PEG 400 and paraffin[51,52]. This observation suggests that these particular nanoparticles can structure PEG 400 through both mechanisms and paraffin through attractive physical interactions between hydrophobised silica surfaces.

These observations highlight that the rational selection of a non-aqueous polar–apolar phase pair, guided by solubility descriptors such as Hildebrand parameters, together with the use of intermediate-polarity nanoparticles, provides a robust formulation strategy. This design approach could be extended to develop novel Pickering emulsions incorporating higher-melting dispersed phases, thereby enabling phase-change systems suitable for thermal-energy-storage applications operating well above the boiling point of water.

3.3.2. *Viscous flow behaviour of emulsions*

Fig. 5 presents the evolution of viscosity as a function of the shear rate for the PCMEs with different nanoparticle concentrations, together with their raw materials, at 80 °C and 25 °C. The neat phases, as previously discussed, exhibited a Newtonian behaviour, which is characterised by the independence of the viscosity with the shear rate. In contrast, nanoparticle-stabilized PCMEs, across the entire concentration range, displayed a typical flow behaviour of structured systems, at both temperatures. Thus, their flow response is marked by an initial zero-shear viscosity plateau, at low shear rates, followed by a significant viscosity reduction as shear rate increases (shear-thinning region) and, ultimately, a limiting viscosity region at high shear rates.

As shown in Fig. 5, the viscosity of the PCMEs increased with rising silica concentration, mirroring the structuration behaviour previously

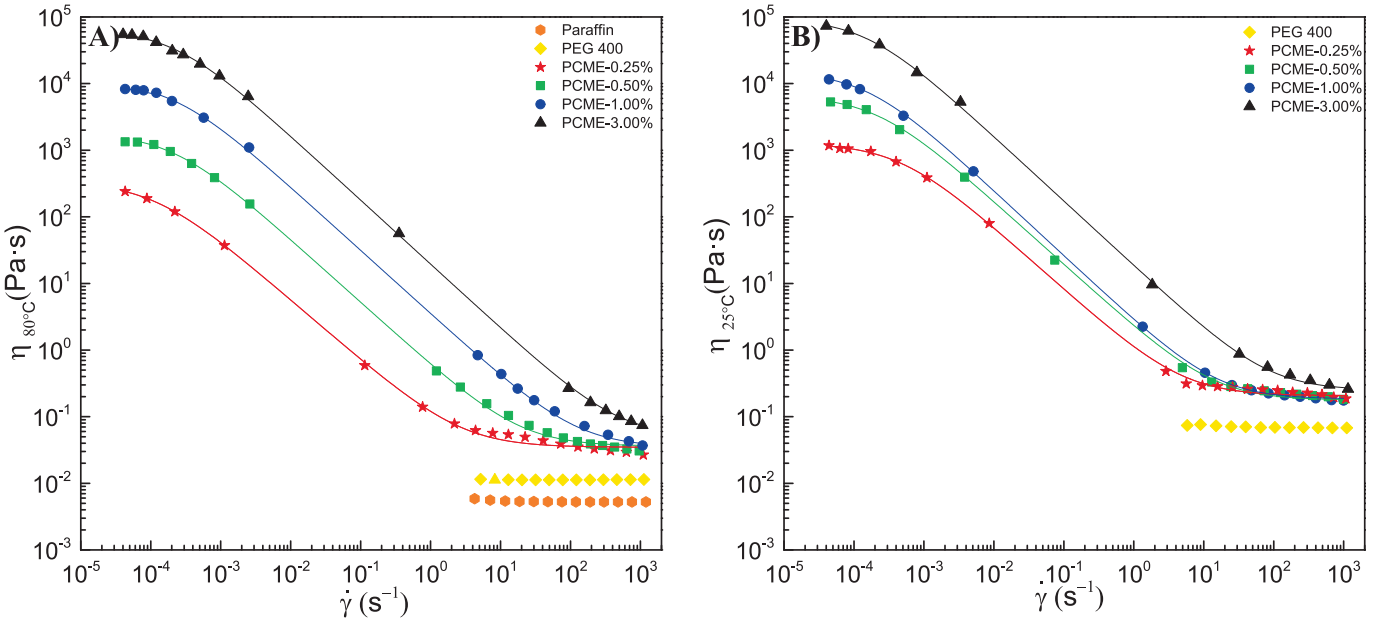

Fig. 5. Effect of nanoparticles concentration on the viscosity of PCMEs. Flow curves of pure PEG 400, pure paraffin and PCMEs at A) 80 °C and B) 25 °C. The solid lines represent the fitting curves obtained using Equation (3).

observed in binary mixtures (Fig. 4). The excess nanoparticle content leads to their presence in the continuous phase, where they partially contribute to the developed structure and thereby enhance flow resistance[51,63]. Thus, as it has already be mentioned, nanoparticles are not only located at the interface but also dispersed causing a thickening behaviour throughout the formation of particle networks [88,89], and together with the densely packed droplet assembly produced at higher stabilizer contents, can partially explain viscosity rise with nanoparticle addition. This effect positively influences emulsion stability by inducing steric stabilization[65]. Notably, comparison of Fig. 4 and Fig. 5 reveals that the emulsion viscosities are only slightly higher than those of the corresponding binary mixtures at the same silica concentration. This fact indicates that the increase in viscosity is predominantly attributable to the presence of dispersed nanoparticles within the continuous phase, which leads to a network-like structuration process driven by interactions between hydrophobised silica surfaces, as observed in the binary mixtures[37]. Besides that, viscosity was additionally increased as a result of the formation of disperse-phase droplets and their physical interactions, as expected in emulsions[90]. Moreover, the progressive decrease of the average droplet size (see Table 1) also contributes the enhanced viscosity, since the growth of the droplet superficial area enhances the droplet forces interaction, promoting fluidity resistance [51,88,91]. At higher shear rates, the observed strong shear-thinning response towards constant values is often attributed to the shear-induced deflocculation process of the highly structured system, particularly at high nanoparticles concentration, breakdown of particle networks and droplet deformation and alignment[67]. These mechanisms explain why the viscosity of the emulsions closely tracks that of the corresponding binary mixtures, with additional contributions arising from droplet deformation and interfacial crowding.

Although the reported increase in viscosity may be seen as a drawback for transportation of PCMEs, the high shear rates typically encountered in pumping operations (>10 s^{-1}), led to a strong reduction in viscosity. Consequently, for in-service applications such as heat transfer fluids, this high sensitivity of emulsion viscosity to shear offers a practical advantage by reducing the required pumping power during transport. Nonetheless, for other applications, the controlled viscosity enhancement through precise nanoparticle dosage can be beneficial in addition to improving emulsion stability, which is a key factor in PCME performance.

On the other hand, Fig. 5 also highlights the influence of temperature on the emulsions' viscosity, as shown by the flow curves of PCMEs at both 80 °C (Fig. 5**A**)) and 25 °C (Fig. 5 (B)). As expected, lower temperatures led to an increase in viscosity, due to the phase transition of paraffin droplets from a liquid state, at 80 °C, to a solid state, at 25 °C, since paraffin crystals are less prone to be deformed under shear stress compared to liquid droplets[92]. Additionally, reduced molecular mobility and increased internal friction, at lower temperatures, further contribute to the overall viscosity enhancement of the system. Interestingly, emulsions with higher nanoparticle concentrations exhibited a comparatively smaller increase in viscosity upon cooling. This phenomenon can be attributed to the enhanced structural stability imparted by the excess nanoparticles dispersed within the continuous phase. These silica particles create a more robust network, which not only contributes to the stabilization of the emulsion but also mitigates the increase in viscosity that typically accompanies the solidification of the paraffin droplets[51,52,67].

To further analyse the viscosity flow curves, the viscosity data in Fig. 5 were successfully fitted to the Cross equation (**Equation (3)**[93], a widely used model for pseudoplastic flow associated with the formation and disruption of internal structures[94]:

$$\eta = \eta_\infty + \frac{\eta_0 - \eta_\infty}{1 + (\lambda\dot{\gamma})^P} \tag{3}$$

where η represents the apparent viscosity (Pa·s); η_∞ is the infinite-shear viscosity (Pa·s); η_0 is the zero-shear limiting viscosity (Pa·s); λ is a time constant (s) associated with the shear-dependent structural breakdown, whose reciprocal defines the characteristic shear rate at which the transition from the Newtonian plateau (η_0) to the shear-thinning regime begins, $\dot{\gamma}$ is the shear rate (s^{-1}) and P is the shear-thinning index, ranging from 0 (Newtonian behaviour) to 1 (extreme shear thinning). The shear-thinning index *P* is related to the power law index n by the expression n= (1–*P*)[93].

This model provides an accurate representation across the full range of shear rates studied, yielding a high degree of reliability ($R^2 > 0.99$). The parameters obtained from fitting the Cross model to the flow curves provide valuable insight into the structural changes occurring in the emulsions as a function of nanoparticle concentration and temperature. These parameters are gathered in Table 2.

Table 2
Cross model parameters and correlation factors derived from flow curve analysis (Fig. 5).

Sample	η_∞(Pa s)	η_0(Pa·s)	λ(s)	*P*	R^2
Temperature: **80 °C**					
PCME-3.00%	0.050	65834.0	4631.1	0.963	0.993
PCME-1.00%	0.035	11139.0	4755.7	0.952	0.997
PCME-0.50%	0.036	1821.3	4850.2	0.947	0.999
PCME-0.25%	0.035	273.4	4764	0.941	0.991
Temperature: **25 °C**					
PCME-3.00%	0.250	95212.6	6691.5	0.975	0.998
PCME-1.00%	0.185	15094.8	6655.2	0.951	0.999
PCME-0.50%	0.188	6624.1	4696.0	0.949	0.999
PCME-0.25%	0.206	1273.9	2141.1	0.942	0.998

Interestingly, with the exception of the highest nanoparticle concentration, the emulsions tended to reach similar values of η_∞ across the concentration in both temperatures, further highlighting the dominant role of the continuous phase in controlling the flow response of emulsions. The λ parameter exhibited two distinct trends depending on the phase state of the paraffin. Thus, at 80 °C, when the paraffin is in the molten state, λ values remained relatively constant regardless of silica concentration. In contrast, at 25 °C, when the paraffin is solidified, λ increased with nanoparticle concentration. Since higher λ values indicate a greater shear-dependent contribution to structural breakdown [93], these results–together with the η_0 evolution–point out microstructure development is promoted by both the crystallization of the disperse phase and the nanoparticle content. Indeed, other authors have reported that the elongated shape of frozen paraffin droplets (Fig. 3 (A 2,3-E2,3)) in crystallisable emulsions may lead to the formation of three-dimensional structures without inducing coalescence, which would restrict emulsion flow[77,79,95]. However, the presence of nanoparticles at the droplet interface, and particularly within the continuous phase, may further contribute to structural organization and mitigate the impact of the droplets' geometrical constraints on the flow, thereby supporting the observed shear-thinning response[78]. Finally, the high values of *P* (approaching 1) are consistent with the strong shear-thinning characteristics observed. In general, the values of the Cross-model parameters indicate that the developed microstructures are highly sensitive to shear stress.

In order to better understand structural effects, the zero-shear limiting viscosity (η_0) of both emulsions and their corresponding binary mixtures of PEG with nanoparticles was plotted as a function of the nanosilica concentration, at 25 and 80 °C (Fig. 6). As shown, η_0 values for the emulsions underwent a remarkable increase of several orders of magnitude compared with those of the continuous phase alone (i.e. at 0 wt% nanoparticles). Interestingly, the single addition of nanoparticles to the continuous phase, PG-NP, also yielded a similar trend, pointing out their previously commented strong structuring effect. In contrast, the effect of the crystallization of the disperse phase, i.e., its solidification, results in only a minor additional rise, highlighting its limited contribution to the overall microstructure. Notably, η_0 values tend to converge with those of the binary mixtures, suggesting that the effect of temperature becomes less pronounced as nanoparticle concentration increase.

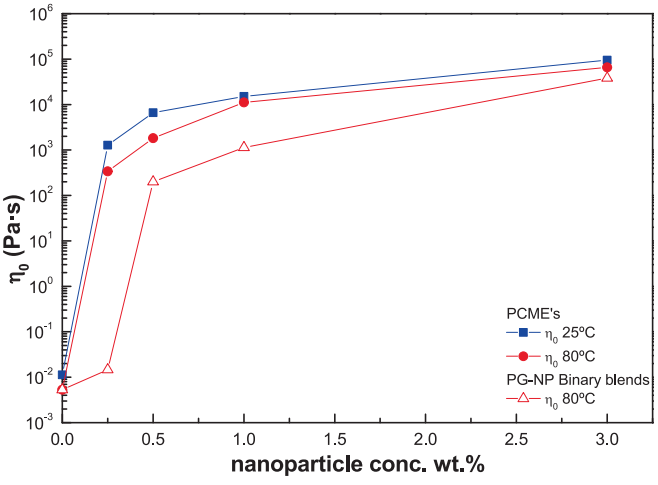

Fig. 6. Evolution of the zero-shear limiting viscosity of the PCMEs and PG-NP binary blends with nanoparticle concentration and different temperatures (80 °C and 25 °C).

3.3.3. *Dynamic tests of emulsions*

Dynamic rheological testing is a powerful tool for characterizing the viscoelastic properties of emulsions, providing valuable insights into their structural integrity. Oscillatory frequency sweep tests are particularly effective in assessing the internal micro-nanostructure, the extent of droplet interactions and the role of stabilizers within the emulsions.

The results of the storage modulus (G′) and loss modulus (G″) as functions of angular frequency for PCMEs with varying nanoparticles concentrations are shown in Fig. 7 at both 25 and 80 °C.

At both temperatures, a rubbery plateau region was observed across the evaluated angular frequency range, where G′ exhibited a well-defined plateau with values consistently higher than G″, which reached a minimum at intermediate or low frequencies. These characteristics indicate that emulsions predominantly exhibit elastic behaviour, confirming the formation of gel-like structures[96].

In addition, the width of the rubbery plateau region tended to be reduced as temperature increased and nanosilica content lowered, as evidenced by the appearance of a crossover point in the high-frequency region, particularly at 80 °C. This trend is consistent with a transition from weaker entangled network structures in PCMEs with less than 0.5 wt% stabilizer to stronger gel-like structures as the availability of nanoparticles increases [97,98].

The dynamic response of the PCMEs can be understood by considering the collective contribution of the droplet interactions and the nanoparticle network. The dominance of G′ over G″ indicates that the system stores more mechanical energy than it dissipates during deformation, which is characteristic of structured viscoelastic materials. This behaviour is consistent with the presence of a three-dimensional microstructure composed of interfacial particle layers adsorbed at the droplet interface, together with excess hydrophobized silica dispersed throughout the continuous phase that further reinforces this network. These structures give rise to the rubbery plateau typically observed in structured colloidal gels. As the nanoparticle concentration increases, the reduced interparticle distance and enhanced attractive interactions further consolidate this network, explaining the systematic rise in both the elastic (G′) and viscous (G″) contributions [51].

In line with the temperature-dependent viscosity behaviour, both G′ and G″ moduli increased only marginally after the crystallization of the dispersed phase, with a more pronounced effect in samples with lower nanoparticle content. This agrees with the formation of three-dimensional structures of rough and elongated paraffin crystals [77–79] at a microscale level within a continuous phase of nanoparticles dispersed at the nanoscale, which also forms a three-dimensional nanonetwork. Therefore, both structures provide elasticity to the system and contribute significantly to increasing viscosity and internal friction (Fig. 6 and Fig. 7). Consequently, the well-established three-dimensional network formed by the excess of nanoparticles could effectively cushion the impact of paraffin crystallization on the rheological properties[78]. As a result, both moduli do not show a notable increase, as the nanoparticle network predominantly governed the structural properties, minimizing additional reinforcement from the solidified paraffin phase. In such cases, the limited effect of paraffin crystallization on G′ and G″, particularly at higher stabilizer contents, indicates that the nanoparticle network largely governs the elasticity of

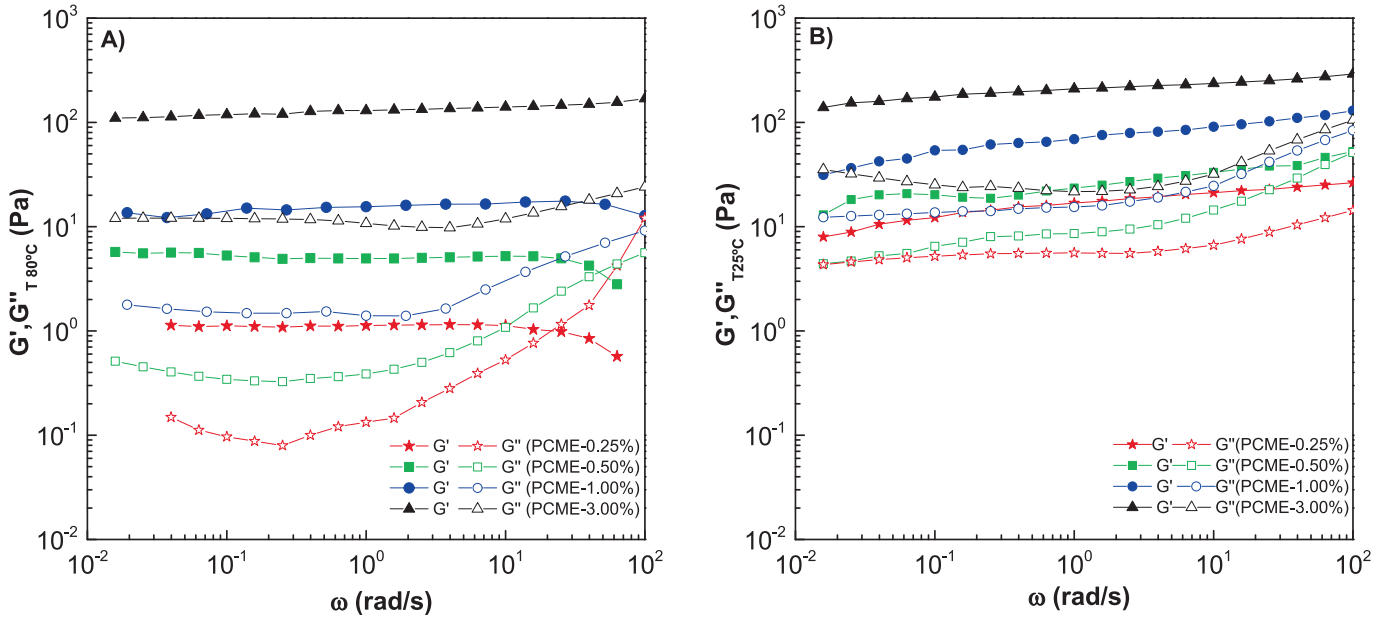

Fig. 7. Storage (G′) and loss modulus (G″) as a function of frequency of the emulsions at different nanoparticle concentrations and different temperatures: **A)** 80 °C, **B)** 25 °C.

the system, effectively buffering the mechanical reinforcement usually associated with droplet solidification.

3.4. Thermo-physical properties and energy storage performance

Thermal behaviour of the pure components, binary mixtures, and PCMEs was analysed using modulated differential scanning calorimetry (MDSC). Their corresponding thermograms are presented in Fig. 8 and their key thermal properties are summarized in Table 3.

The MDSC curve of paraffin exhibited major melting and crystallization points at 58.3 °C and 56.9 °C, with corresponding total enthalpy values of 190.9 J/g and 191.2 J/g, respectively (Fig. 8 and Table 3). These results align well with the literature, indicating a minimal supercooling effect (temperature difference between melting and crystallization) for this type of paraffin[17,99]. It is also worth mentioning that the MDSC curves of pure paraffin displayed secondary peaks in both the heating and cooling scans at temperatures lower than the main event. This is a frequently reported thermal behaviour for n-alkanes an paraffin waxes, where the minor peak relates to solid phase transitions and the formation of intermediate rotator phases, followed by complete melting of the crystalline structure[100–102].

As previously discussed, the partial compatibility of nanoparticles with both phases suggests that their presence in the dispersed phase could influence the phase change process, particularly crystallization. To explore this effect, a binary blend of paraffin and nanosilica (PF-NP-1%) was also analysed and presented in Fig. 8 **(A)**. The blend exhibited transition peaks virtually identical to those of neat paraffin, indicating that the stabilizer did not affect the crystallinity of paraffin. This represents an improvement compared to the silicon-based surfactant, according to previous findings by our research group, where stabilizers

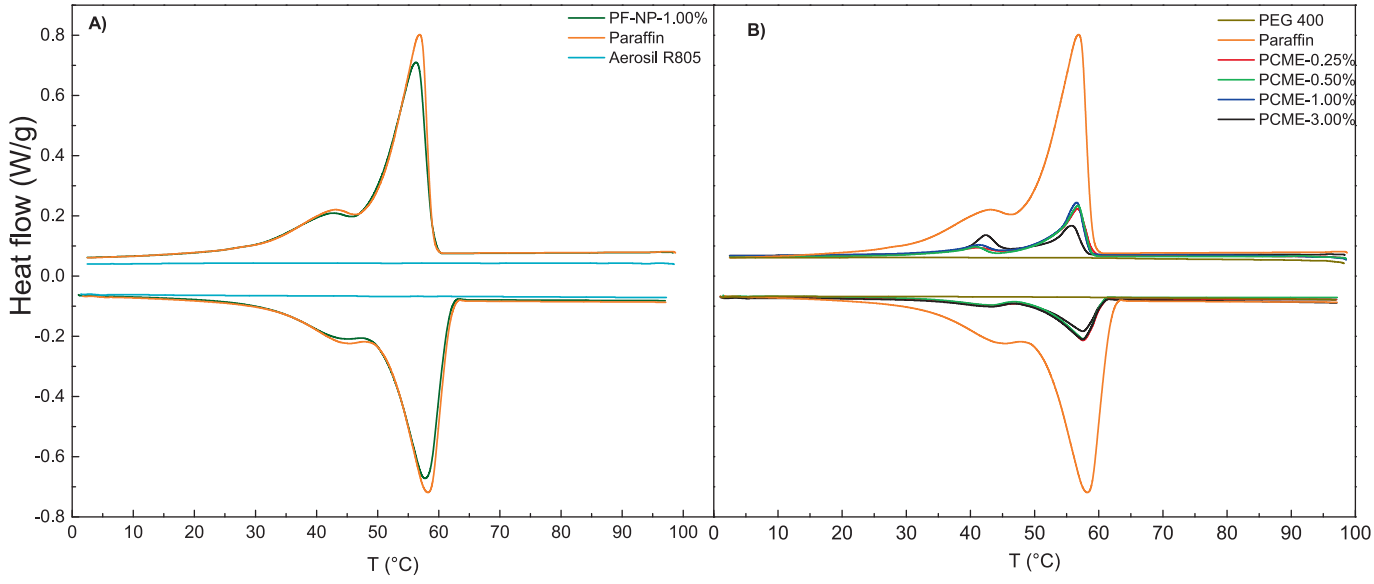

Fig. 8. MDSC thermograms for **A**) Paraffin, Aerosil R-805, and a paraffin/nanoparticle blend (PF-NP-1.00%). **B)** PCMEs, PEG400 and paraffin.

Table 3
Thermal properties of the PCMEs and pure paraffin from MDSC analysis.

Sample	Crystallization				Melting				Supercooling
	T_c^{Peak} (°C)	T_c^{Onset} (°C)	$\Delta H_c (J/g)$	$\Delta H_{c(n)}$ [a] (J/gPF)	T_m^{Peak} (°C)	T_m^{Onset} (°C)	$\Delta H_m (J/g)$	$\Delta H_{m\,(n)}$ [b] (J/gPF)	ΔT °(C)
PCME-0.25%	56.7	59.0	34.80	174.0	57.6	50.6	33.34	166.69	0.9
PCME- 0.50%	56.7	58.8	34.53	172.7	57.6	50.3	33.03	165.15	0.8
PCME- 1.00%	56.6	58.4	33.73	168.6	57.5	50.1	32.94	164.69	0.9
PCME- 3.00%	55.8	58.0	31.44	157.2	58.2	49.9	31.79	158.95	2.4
Paraffin	56.9	58.9	190.89	190.9	58.2	50.1	191.22	193.12	1.4

a: $\Delta H_{c\,(n)}$ corresponds to the crystallization enthalpy normalized by the mass fraction of paraffin in the emulsion.
b: $\Delta H_{m\,(n)}$ corresponds to the melting enthalpy normalized by the mass fraction of paraffin in the emulsion.

negatively influenced the crystallinity of the PCM[32].

Interestingly, all previously identified transition peaks of paraffin were also observed in the MDSC curves of the emulsions. Moreover, the enthalpy values per gram of dispersed phase ($\Delta H_{m\,(n)}$ and $\Delta H_{C\,(n)}$) remain consistent with those of bulk paraffin, confirming that neither the emulsion components nor the emulsification process adversely affected paraffin crystallinity. These observations indicate that the internal crystalline structure of the PCM remains largely unaltered, enabling reliable qualitative assessment of its thermal behaviour within the emulsion.

Supercooling is one of the main drawbacks in developing phase-change emulsions because it delays the phase change and reduces system efficiency[101]. This phenomenon in PCMEs is mainly attributed to the transition from heterogeneous to homogeneous nucleation, which is more pronounced with smaller droplet size, further reducing the homogeneous nucleation rate. In PCMEs, the crystallization of dispersed droplets can occur separately in each droplet volume due to their small size, typically resulting in a higher degree of supercooling compared to bulk paraffin[103]. In addition, the presence of surfactants influences the interfacial properties, modify surface energy, and thereby either promote or suppress nucleation. In addition to the supercooling, the emulsification process frequently lowers the crystallinity of the dispersed PCM. This reduction can be attributed to two main factors. First, the confinement of droplets restricts molecular mobility, hindering the long-range ordering of chains during crystallization. Second, the partial compatibility of the dispersed phase with the emulsifier, along with the emulsifier's presence at the droplet interface, can disrupt crystal growth by altering interfacial energy and impeding molecular packing. Consequently, PCMEs typically exhibit lower enthalpies of fusion compared to their bulk counterparts [99].

Nonetheless, as can be seen in Table 3, the emulsification process had only a minor impact on the enthalpies and transition temperatures of the studied PCMEs, with minimal influence from the previously mentioned phenomena—whether positive, such as nucleating effects, or negative, such as compatibilization between phases. Since the intermediate-polarity nanoparticles exhibit partial compatibility with the molten PCM, their adsorption at the droplet interface produces a rigid particulate layer that does not significantly interfere with molecular mobility within the droplet core. As a result, paraffin molecules retain sufficient freedom to undergo the liquid–solid transition with crystallization pathways similar to those of the bulk material, explaining the preservation of melting and crystallization enthalpies. Only the sample with the highest nanoparticle concentration showed a slight increase in supercooling and a small reduction in phase enthalpy, which can be attributed to the decreased droplets size and the previously mentioned effects in crystallization.

To evaluate thermal storage capacity, Table 4 compares the phase change enthalpy (ΔH_m) values for various aqueous paraffin-based PCM emulsions reported in the literature, with the same dispersed phase concentration (20 w/w%), to the present anhydrous Pickering PCM emulsion. For consistency, the percentage difference in ΔH_m between the neat paraffin and the emulsions was calculated. The results show

Table 4
Melting enthalpies for different paraffin-based emulsions.

Type	System (PCM + stabilizer)	Bulk PCM $\Delta H_m (J/g)$	Emulsion (20 wt% PCM) $\Delta H_m (J/g)$	% Difference
o/w	Paraffin (16–17 °C) – Polyethylene glycol dodecyl ether + polysorbate [115]	244.75	41.31	0.83
	Paraffin (60 °C)- polysorbate [116]	253.91	48.63	0.80
	Paraffin (62–64 °C) – PVA and PEG-600[117]	211.80	42.10	0.80
o/o	Paraffin (58–60 °C)- hydrophobic silica nanoparticles (0.5%)	190.89	33.37	0.82

that all the systems exhibit relatively similar ΔH_m values, indicating that the thermal storage capacity of the present oil-in-oil Pickering PCME is comparable to that of well-established surfactant-stabilized aqueous emulsions. This suggests that the Pickering emulsion formulation preserves the effective energy storage potential typical of PCM systems, maintaining phase change enthalpy even with a different stabilization mechanism. Therefore, it demonstrates strong potential as a competitive alternative for thermal energy storage applications.

In addition to their latent heat storage capacity, efficient phase-change materials must exhibit favourable thermal transport properties that contribute to overall thermal energy-storage performance. A key parameter is also the thermal conductivity, as it directly governs the rate at which heat can be absorbed and released during melting and solidification. Several strategies have been proposed to control and to enhance the inherently low thermal conductivity of PCMs, including the incorporation of nanoparticles, the use of porous skeletons, and micro-encapsulation [104–106]. Silica nanoparticles have been widely used as thermal conductivity modifiers in various applications. They can act as insulating additives due to their high porosity and nanoscale structure [107,108]; however, they may also enhance heat transfer when they connect to form a three-dimensional spatial network, creating multiple thermal conduction pathways [109]. Therefore, evaluating the thermal

Table 5
Evolution of thermal conductivity with testing temperature for raw materials, a selected binary blend and PCMEs.

Sample	k ($W \cdot m^{-1} \cdot K^{-1}$) 25 °C	80 °C
Paraffin	0.233	0.185
PEG 400	0.195	0.196
PG-NP-3.00%	0.194	0.197
PCME-0.25%	0.213	0.191
PCME-0.50%	0.213	0.192
PCME-1.00%	0.214	0.194
PCME-3.00%	0.212	0.192

conductivity of the developed systems is essential to understand the influence of these components on heat-transfer behaviour.

Table 5 presents the thermal conductivity of paraffin wax, PEG 400, the reference binary blend, and the emulsions at selected temperatures (25 °C and 80 °C). Thermal conductivity values of PEG 400 are in a good agreement with literature [110] and does not exhibit significant changes with temperature. Interestingly, the incorporation of hydrophobized fumed silica nanoparticles did not significantly alter the thermal conductivity of PEG, as the binary blend exhibited nearly identical values. Although rheological tests revealed a certain degree of microstructuration in the PEG matrix due to physical interactions between the nanoparticles, the concentrations evaluated appear insufficient to induce a measurable change in its thermal conductivity. These results are consistent with similar studies, which reported the dependence of thermal conductivity on particle concentration [111].

In contrast, paraffin exhibited a pronounced decrease in thermal conductivity with increasing temperature, a behaviour characteristic of its solid–liquid phase transition. The thermal conductivity values measured for paraffin in the solid state are consistent with those reported for paraffinic materials of similar melting point, which typically fall within the 0.15–0.35 $W\ m^{-1}\ K^{-1}$ range [112,113]. Because the effective thermal conductivity of emulsions depends on the intrinsic properties of both phases and their respective volume fractions [114], the PCMEs are expected to display an intermediate trend. At lower temperatures, the PCMEs show higher thermal conductivity than PEG 400 alone, reflecting the contribution of solid paraffin, whose conductivity exceeds that of the continuous phase. Conversely, once paraffin is fully melted, the emulsions exhibit lower thermal conductivity, consistent with the substantially reduced conductivity of liquid pristine paraffin and in agreement with trends reported for comparable paraffin-based systems.

Finally, and consistent with the behaviour of the binary blend, increasing the nanoparticle concentration up to 3 wt% did not significantly affect the thermal conductivity of the PCMEs. Although higher nanoparticle concentration loadings than the presented in this work could potentially enhance thermal conductivity and therefore improve heat exchange rates, they would also significantly increase the viscosity of the system, leading to higher pumping energy requirements. Further work is therefore required to explore strategies to increase thermal conductivity without compromising the rheological behaviour of these systems.

4. Conclusions

Hydrophobised fumed silica nanoparticles successfully stabilise oil-in-oil paraffin-in-PEG400 emulsions with a dispersed phase concentration of 20 wt% when the stabiliser concentration exceeds 0.1 wt%. Optical microscopy of the emulsions revealed a homogeneous distribution of spherical droplets throughout the continuous phase, which exhibited a slight deviation in circularity following paraffin crystallisation. Increasing stabilizer concentration led to a reduction in droplet size and the progressive formation of network-like structures. As a consequence of the resulting structure, the linear viscoelastic behaviour of PCMEs displayed a gel-like response, which was enhanced with nanoparticle content.

At both 25 °C and 80 °C, the PCMEs displayed flow behaviour characteristic of structured systems, including a Newtonian plateau at low shear rates, followed by shear-thinning and an infinite-shear viscosity region. Higher nanoparticle contents led to an increase in zero-shear viscosity, whereas the systems tended to converge towards similar limiting viscosity values at high shear rates. Additionally, comparison of the flow curves of PCMEs and their corresponding binary blends revealed that an excess of hydrophobised fumed silica was distributed throughout the continuous phase, leading to a pronounced structuring effect. This effect is sufficiently strong to dampen the mechanical response associated with the solidification of the dispersed paraffin phase during its crystallisation, as the temperature decreases from 80 °C to 25 °C. This dependency on nanoparticle concentration can thus serve as a useful formulation tool, as adjusting the silica content enables control over the rheological properties of the emulsion for specific applications.

In general, the rheological behaviour was associated with a complex, multi-level structure. At the microscale, a three-dimensional network formed by the dispersed paraffin phase (solid at 25 °C and liquid at 80 °C) is embedded within a continuous phase containing nanoparticles dispersed at the nanoscale, which themselves organize into a secondary three-dimensional nanonetwork.

Thermal analysis showed that hydrophobized fumed silica presented minimal effect on the thermal properties and low supercooling phenomena of the emulsions. The phase change enthalpy was comparable with other aqueous paraffin-based systems found. Moreover, micrographics did not show significant changes in the size and shape of the paraffin droplets after a cooling and reheating process, indicating a suitable thermal stability.

Taken together, the morphological, rheological, and thermal results demonstrate that the formulation strategy developed in this work provides a robust foundation for scaling up oil-in-oil Pickering emulsions with favourable thermophysical behaviour. The combination of a polar–apolar phase pair with intermediate-polarity nanoparticles proved effective for producing well-structured emulsions, underscoring its potential as a versatile approach for designing next-generation systems. This formulation strategy could be further extended to incorporate higher-melting phase-change materials, enabling thermal-energy-storage systems capable of operating at temperatures well above the boiling point of water. Moreover, the present findings highlight the importance of optimising key properties such as latent-heat storage capacity and thermal conductivity to enhance the overall performance of high-temperature PCME formulations.

CRediT authorship contribution statement

Sebastián Sanabria: Writing – original draft, Investigation, Data curation. **Clara Delgado-Sánchez:** Writing – review & editing, Methodology, Investigation. **Adrián Tenorio-Alfonso:** . **Antonio A. Cuadri:** Methodology, Data curation. **Francisco Javier Navarro:** Writing – review & editing, Validation, Data curation, Conceptualization.

Declaration of competing interest

The authors declare that they have no known competing financial interests or personal relationships that could have appeared to influence the work reported in this paper.

Acknowledgments

This work is part of the projects PID2023-151306OB-I00 and PDC2025-166144-I00 funded by MICIU/AEI /10.13039/501100011033 and by FEDER, EU. Adrián Tenorio and Clara Delgado also acknowledge financial support from Junta de Andalucía through the post-doctoral Grants POSTDOC_21_00644 and EMERGIA DGP_E-MEC_2023_00091, respectively. Funding for open access charge: Universidad de Huelva / CBUA.

Data availability

Data will be made available on request.

References

[1] A. Shukla, D. Buddhi, R.L. Sawhney, Solar water heaters with phase change material thermal energy storage medium: a review, Renew. Sustain. Energy Rev. 13 (2009) 2119–2125, https://doi.org/10.1016/j.rser.2009.01.024.

[2] G. Zhang, Z. Yu, G. Cui, B. Dou, W. Lu, X. Yan, Fabrication of a novel nano phase change material emulsion with low supercooling and enhanced thermal conductivity, Renew. Energy 151 (2020) 542–550, https://doi.org/10.1016/j.renene.2019.11.044.
[3] K. Chinnaiyan, D. Prakash, Review on phase Change Materials with Nanoparticle in Engineering applications, Journal of Engineering Science and Technology Review 9 (2016) 26–36, https://doi.org/10.25103/jestr.094.05.
[4] B. Zalba, J.M. Marín, L.F. Cabeza, H. Mehling, Review on thermal energy storage with phase change: materials, heat transfer analysis and applications, Appl. Therm. Eng. 23 (2003) 251–283, https://doi.org/10.1016/S1359-4311(02)00192-8.
[5] A.H. Abedin, A Critical Review of Thermochemical Energy Storage Systems, TOREJ 4 (2011) 42–46, https://doi.org/10.2174/1876387101004010042.
[6] D.N. Nkwetta, F. Haghighat, Thermal energy storage with phase change material—A state-of-the art review, Sustain. Cities Soc. 10 (2014) 87–100, https://doi.org/10.1016/j.scs.2013.05.007.
[7] F. Wang, W. Lin, Z. Ling, X. Fang, A comprehensive review on phase change material emulsions: Fabrication, characteristics, and heat transfer performance, Sol. Energy Mater. Sol. Cells 191 (2019) 218–234, https://doi.org/10.1016/j.solmat.2018.11.016.
[8] F. Souayfane, F. Fardoun, P.-H. Biwole, Phase change materials (PCM) for cooling applications in buildings: a review, Energ. Buildings 129 (2016) 396–431, https://doi.org/10.1016/j.enbuild.2016.04.006.
[9] D. Cabaleiro, F. Agresti, L. Fedele, S. Barison, C. Hermida-Merino, S. Losada-Barreiro, S. Bobbo, M.M. Piñeiro, Review on phase change material emulsions for advanced thermal management: Design, characterization and thermal performance, Renew. Sustain. Energy Rev. 159 (2022) 112238, https://doi.org/10.1016/j.rser.2022.112238.
[10] M. Delgado, A. Lázaro, J. Mazo, B. Zalba, Review on phase change material emulsions and microencapsulated phase change material slurries: Materials, heat transfer studies and applications, Renew. Sustain. Energy Rev. 16 (2012) 253–273, https://doi.org/10.1016/j.rser.2011.07.152.
[11] J. Shao, J. Darkwa, G. Kokogiannakis, Review of phase change emulsions (PCMEs) and their applications in HVAC systems, Energ. Buildings 94 (2015) 200–217, https://doi.org/10.1016/j.enbuild.2015.03.003.
[12] J. Ji, C. Zhang, S. Cai, X. Zhang, H. Tong, Research progress of stability and supercooling in phase change material emulsions, Int. J. Refrig 168 (2024) 159–177, https://doi.org/10.1016/j.ijrefrig.2024.08.015.
[13] P. O'Neill, L. Fischer, R. Revellin, J. Bonjour, Phase change dispersions: a literature review on their thermo-rheological performance for cooling applications, Appl. Therm. Eng. 192 (2021) 116920, https://doi.org/10.1016/j.applthermaleng.2021.116920.
[14] P. Schalbart, M. Kawaji, K. Fumoto, Formation of tetradecane nanoemulsion by low-energy emulsification methods, Int. J. Refrig 33 (2010) 1612–1624, https://doi.org/10.1016/j.ijrefrig.2010.09.002.
[15] T. Morimoto, H. Kumano, Flow and heat transfer characteristics of phase change emulsions in a circular tube: Part 1. Laminar flow, Int. J. Heat Mass Transf. 117 (2018) 887–895, https://doi.org/10.1016/j.ijheatmasstransfer.2017.10.055.
[16] J. Chen, P. Zhang, Preparation and characterization of nano-sized phase change emulsions as thermal energy storage and transport media, Appl. Energy 190 (2017) 868–879, https://doi.org/10.1016/j.apenergy.2017.01.012.
[17] M.M. Kenisarin, Thermophysical properties of some organic phase change materials for latent heat storage, A Review, Solar Energy 107 (2014) 553–575, https://doi.org/10.1016/j.solener.2014.05.001.
[18] D. Cabaleiro, S. Losada-Barreiro, F. Agresti, C. Hermida-Merino, L. Fedele, L. Lugo, S. Barison, M.M. Piñeiro, Development and Thermophysical Profile of Cetyl Alcohol-in-Water Nanoemulsions for thermal Management, Fluids 7 (2022) 11, https://doi.org/10.3390/fluids7010011.
[19] Q. Li, G. Qiao, E. Mura, C. Li, L. Fischer, Y. Ding, Experimental and numerical studies of a fatty acid based phase change dispersion for enhancing cooling of high voltage electrical devices, Energy 198 (2020) 117280, https://doi.org/10.1016/j.energy.2020.117280.
[20] J. Allouche, Synthesis of Organic and Bioorganic Nanoparticles: An Overview of the Preparation Methods, in: R. Brayner, F. Fiévet, T. Coradin (Eds.), Nanomaterials: A Danger or a Promise? A Chemical and Biological Perspective, Springer, London, 2013: pp. 27–74. doi:10.1007/978-1-4471-4213-3_2.
[21] J. Feng, J. Huang, Z. Ling, X. Fang, Z. Zhang, Performance enhancement of a photovoltaic module using phase change material nanoemulsion as a novel cooling fluid, Sol. Energy Mater. Sol. Cells 225 (2021) 111060, https://doi.org/10.1016/j.solmat.2021.111060.
[22] H. Liang, L. Liu, Z. Zhong, Y. Gan, J.-Y. Wu, J. Niu, Towards idealized thermal stratification in a novel phase change emulsion storage tank, Appl. Energy 310 (2022) 118526, https://doi.org/10.1016/j.apenergy.2022.118526.
[23] J. Luo, H. Gu, S. Wang, H. Wang, D. Zou, A coupled power battery cooling system based on phase change material and its influencing factors, Appl. Energy 326 (2022) 119917, https://doi.org/10.1016/j.apenergy.2022.119917.
[24] C. Wei, J. Shao, J. Darkwa, Experimental investigations into thermal performance of phase change emulsion in a fin-and-tube heat exchanger, Int J Low-Carbon Tech 18 (2023) 175–183, https://doi.org/10.1093/ijlct/ctad001.
[25] Cooling performance of mini-channel heat sink with water-based nano-PCM emulsion-An experimental study - ScienceDirect, (n.d.). https://www.sciencedirect.com/science/article/pii/S1290072921000703 (accessed January 9, 2025).
[26] L. Liu, J. Li, J. Niu, J.-Y. Wu, Evaluation of the energy storage performance of PCM nano-emulsion in a small tubular heat exchanger, Case Stud. Therm. Eng. 26 (2021) 101156, https://doi.org/10.1016/j.csite.2021.101156.
[27] A. Yaqoob Khan, S. Talegaonkar, Z. Iqbal, F. Jalees Ahmed, R. Krishan Khar, Multiple Emulsions: An Overview, Current Drug Delivery 3 (2006) 429–443, https://doi.org/10.2174/156720106778559056.
[28] A. Zia, E. Pentzer, S. Thickett, K. Kempe, Advances and Opportunities of Oil-in-Oil Emulsions, ACS Appl. Mater. Interfaces 12 (2020) 38845–38861, https://doi.org/10.1021/acsami.0c07993.
[29] C. Delgado-Sánchez, A.A. Cuadri, F.J. Navarro, P. Partal, Formulation and processing of novel non-aqueous polyethylene glycol-in-silicone oil (o/o) phase change emulsions, Sol. Energy Mater. Sol. Cells 221 (2021) 110898, https://doi.org/10.1016/j.solmat.2020.110898.
[30] C. Delgado-Sánchez, P. Partal, M.J. Martín-Alfonso, F.J. Navarro, Oil-in-Oil emulsions of stearic acid dispersed in silicone oil with enhanced energy storage capability for heat transfer fluids, Sol. Energy Mater. Sol. Cells 245 (2022) 111893, https://doi.org/10.1016/j.solmat.2022.111893.
[31] D. Crespy, K. Landfester, Making dry fertile: a practical tour of non-aqueous emulsions and miniemulsions, their preparation and some applications, Soft Matter 7 (2011) 11054–11064, https://doi.org/10.1039/C1SM06156A.
[32] C. Delgado-Sánchez, P. Partal, M.J. Martín-Alfonso, F.J. Navarro, Role of crystallinity on the thermal and viscous behaviour of polyethylene glycol-in-silicone oil (o/o) phase change emulsions, J. Ind. Eng. Chem. 103 (2021) 348–357, https://doi.org/10.1016/j.jiec.2021.08.003.
[33] Y. He, C. Wang, Y. Liu, J. Chen, Y. Wei, G. Chen, Pickering emulsions stabilized by cellulose nanofibers with tunable surface properties for thermal energy storage, Int. J. Biol. Macromol. 280 (2024) 136013, https://doi.org/10.1016/j.ijbiomac.2024.136013.
[34] G. Bahsi Kaya, Y. Kim, K. Callahan, S. Kundu, Microencapsulated phase change material *via* Pickering emulsion stabilized by cellulose nanofibrils for thermal energy storage, Carbohydrate Polymers 276 (2022) 118745, https://doi.org/10.1016/j.carbpol.2021.118745.
[35] T.D. Dao, H.M. Jeong, A Pickering emulsion route to a stearic acid/graphene core–shell composite phase change material, Carbon 99 (2016) 49–57, https://doi.org/10.1016/j.carbon.2015.12.009.
[36] Y. Yang, Z. Fang, X. Chen, W. Zhang, Y. Xie, Y. Chen, Z. Liu, W. Yuan, An Overview of Pickering Emulsions: Solid-Particle Materials, Classification, Morphology, and applications, accessed April 27, 2023, Front. Pharmacol. 8 (2017), https://www.frontiersin.org/articles/10.3389/fphar.2017.00287.
[37] Y. Chevalier, M.-A. Bolzinger, Emulsions stabilized with solid nanoparticles: Pickering emulsions, Colloids Surf A Physicochem Eng Asp 439 (2013) 23–34, https://doi.org/10.1016/j.colsurfa.2013.02.054.
[38] J. Wu, G.-H. Ma, Recent Studies of Pickering Emulsions: Particles Make the Difference, Small 12 (2016) 4633–4648, https://doi.org/10.1002/smll.201600877.
[39] E. Dickinson, Use of nanoparticles and microparticles in the formation and stabilization of food emulsions, Trends Food Sci. Technol. 24 (2012) 4–12, https://doi.org/10.1016/j.tifs.2011.09.006.
[40] J. Hou, T. Huang, M. Alotaibi, A. AlSofi, Long-Term thermal Stability of Ionic Surfactants for improving Oil Production at High-Salinity High-Temperature Conditions, ACS Omega 9 (2024) 11976–11986, https://doi.org/10.1021/acsomega.3c09734.
[41] T. Sharma, G.S. Kumar, B.H. Chon, J.S. Sangwai, Thermal stability of oil-in-water Pickering emulsion in the presence of nanoparticle, surfactant, and polymer, J. Ind. Eng. Chem. 22 (2015) 324–334, https://doi.org/10.1016/j.jiec.2014.07.026.
[42] O.M. Maithya, X. Zhu, X. Li, S.J. Korir, X. Feng, X. Sui, B. Wang, High-energy storage graphene oxide modified phase change microcapsules from regenerated chitin Pickering Emulsion for photothermal conversion, Sol. Energy Mater. Sol. Cells 222 (2021) 110924, https://doi.org/10.1016/j.solmat.2020.110924.
[43] Q. Zhao, F. He, Q. Zhang, J. Fan, R. He, K. Zhang, H. Yan, W. Yang, Microencapsulated phase change materials based on graphene Pickering emulsion for light-to-thermal energy conversion and management, Sol. Energy Mater. Sol. Cells 203 (2019) 110204, https://doi.org/10.1016/j.solmat.2019.110204.
[44] C. Tan, Y. He, B. Luo, M. Liu, Microencapsulated phase change material with chitin nanocrystals stabilized Pickering emulsion for thermal energy storage, Int. J. Biol. Macromol. 240 (2023) 124374, https://doi.org/10.1016/j.ijbiomac.2023.124374.
[45] D. Yin, L. Ma, J. Liu, Q. Zhang, Pickering emulsion: a novel template for microencapsulated phase change materials with polymer–silica hybrid shell, Energy 64 (2014) 575–581, https://doi.org/10.1016/j.energy.2013.10.004.
[46] S. Xu, M. Du, X. Yu, Z. Zhang, L. Zhou, G. Zhu, J. Militky, D. Kremenakova, G. Zhang, Preparation of photothermal conversion and energy storage microcapsules based on Pickering emulsions with poly (*p*-phenylenediamine) as stabilizer and photothermal materials, J. Storage Mater. 59 (2023) 106564, https://doi.org/10.1016/j.est.2022.106564.
[47] M. Akgün, O. Aydın, K. Kaygusuz, Experimental study on melting/solidification characteristics of a paraffin as PCM, Energ. Conver. Manage. 48 (2007) 669–678, https://doi.org/10.1016/j.enconman.2006.05.014.
[48] L. Huang, C. Doetsch, C. Pollerberg, Low temperature paraffin phase change emulsions, Int. J. Refrig 33 (2010) 1583–1589, https://doi.org/10.1016/j.ijrefrig.2010.05.016.
[49] S. Sharma, H. Kitano, K. Sagara, Phase Change Materials for Low Temperature Solar Thermal Applications, in: 2004. https://www.semanticscholar.org/paper/Phase-Change-Materials-for-Low-Temperature-Solar-Sharma-Kitano/5492cd76932f222b0bb74c5c5331aec45f879fbf (accessed January 12, 2025).
[50] C. Albert, M. Beladjine, N. Tsapis, E. Fattal, F. Agnely, N. Huang, Pickering emulsions: Preparation processes, key parameters governing their properties and

potential for pharmaceutical applications, J. Control. Release 309 (2019) 302–332, https://doi.org/10.1016/j.jconrel.2019.07.003.
[51] S.A. Khan, N.J. Zoeller, Dynamic rheological behavior of flocculated fumed silica suspensions, J. Rheol. 37 (1993) 1225–1235, https://doi.org/10.1122/1.550378.
[52] P. Alaee, M. Kamkar, M. Arjmand, Fumed Silica-based Suspensions for Shear Thickening applications: a Full-Scale Rheological Study, Langmuir 38 (2022) 5006–5019, https://doi.org/10.1021/acs.langmuir.2c00591.
[53] A.A. Minea, State of the Art in PEG-Based Heat transfer Fluids and their Suspensions with Nanoparticles, Nanomaterials 11 (2021) 86, https://doi.org/10.3390/nano11010086.
[54] M.A. Marcos, D. Cabaleiro, M.J.G. Guimarey, M.J.P. Comuñas, L. Fedele, J. Fernández, L. Lugo, PEG 400-based phase Change Materials Nano-Enhanced with Functionalized Graphene Nanoplatelets, Nanomaterials 8 (2018) 16, https://doi.org/10.3390/nano8010016.
[55] C.D. Volpe, S. Siboni, The Wilhelmy method: a critical and practical review, Surf. Innovations 6 (2018) 120–132, https://doi.org/10.1680/jsuin.17.00059.
[56] M.C.M. Sequeira, M.F.V. Pereira, H.M.N.T. Avelino, F.J.P. Caetano, J.M.N. A. Fareleira, Viscosity measurements of poly(ethyleneglycol) 400 [PEG 400] at temperatures from 293 K to 348 K and at pressures up to 50 MPa using the vibrating wire technique, Fluid Phase Equilib. 496 (2019) 7–16, https://doi.org/10.1016/j.fluid.2019.05.012.
[57] T. Okubo, Surface Tension of Structured Colloidal Suspensions of Polystyrene and Silica Spheres at the Air-Water Interface, J. Colloid Interface Sci. 171 (1995) 55–62, https://doi.org/10.1006/jcis.1995.1150.
[58] H. Ma, M. Luo, L.L. Dai, Influences of surfactant and nanoparticle assembly on effective interfacial tensions, Phys. Chem. Chem. Phys. 10 (2008) 2207–2213, https://doi.org/10.1039/B718427C.
[59] B.P. Binks, S.O. Lumsdon, Influence of Particle Wettability on the Type and Stability of Surfactant-Free Emulsions, Langmuir 16 (2000) 8622–8631, https://doi.org/10.1021/la000189s.
[60] B.P. Binks, Particles as surfactants—similarities and differences, Curr. Opin. Colloid Interface Sci. 7 (2002) 21–41, https://doi.org/10.1016/S1359-0294(02)00008-0.
[61] E. Vignati, R. Piazza, T.P. Lockhart, Pickering Emulsions: Interfacial Tension, Colloidal Layer Morphology, and Trapped-Particle Motion, Langmuir 19 (2003) 6650–6656, https://doi.org/10.1021/la034264l.
[62] A.H. Nour, Emulsion Types, Stability Mechanisms and Rheology: A Review, (2018). https://papers.ssrn.com/abstract=3324905 (accessed May 31, 2023).
[63] R. Pal, Effect of droplet size on the rheology of emulsions, AIChE J 42 (1996) 3181–3190, https://doi.org/10.1002/aic.690421119.
[64] D.E. Tambe, M.M. Sharma, Factors Controlling the Stability of Colloid-Stabilized Emulsions: I. an Experimental Investigation, J. Colloid Interface Sci. 157 (1993) 244–253, https://doi.org/10.1006/jcis.1993.1182.
[65] B.P. Binks, S.O. Lumsdon, Catastrophic phase Inversion of Water-in-Oil Emulsions Stabilized by Hydrophobic Silica, Langmuir 16 (2000) 2539–2547, https://doi.org/10.1021/la991081j.
[66] X. Zhang, J. Niu, J.-Y. Wu, Development and characterization of novel and stable silicon nanoparticles-embedded PCM-in-water emulsions for thermal energy storage, Appl. Energy 238 (2019) 1407–1416, https://doi.org/10.1016/j.apenergy.2019.01.159.
[67] J. Chen, R. Vogel, S. Werner, G. Heinrich, D. Clausse, V. Dutschk, Influence of the particle type on the rheological behavior of Pickering emulsions, Colloids Surf A Physicochem Eng Asp 382 (2011) 238–245, https://doi.org/10.1016/j.colsurfa.2011.02.003.
[68] C. Liu, Z. Zheng, C. Xi, Y. Liu, Exploration of the natural waxes-tuned crystallization behavior, droplet shape and rheology properties of O/W emulsions, J. Colloid Interface Sci. 587 (2021) 417–428, https://doi.org/10.1016/j.jcis.2020.12.024.
[69] R. Aveyard, B.P. Binks, J.H. Clint, Emulsions stabilised solely by colloidal particles, Adv. Colloid Interface Sci. 100–102 (2003) 503–546, https://doi.org/10.1016/S0001-8686(02)00069-6.
[70] B. Li, Y. Zhao, X. Chen, Z. Wang, J. Xu, W. Shi, Polymer Crystallization with Configurable Birefringence in double Emulsion Droplets, Macromolecules 55 (2022) 3974–3985, https://doi.org/10.1021/acs.macromol.2c00482.
[71] S. Guttman, Z. Sapir, B.M. Ocko, M. Deutsch, E. Sloutskin, Temperature-Tuned Faceting and Shape changes in Liquid Alkane Droplets, Langmuir 33 (2017) 1305–1314, https://doi.org/10.1021/acs.langmuir.6b02926.
[72] N. Denkov, D. Cholakova, S. Tcholakova, S.K. Smoukov, On the Mechanism of Drop Self-Shaping in Cooled Emulsions, Langmuir 32 (2016) 7985–7991, https://doi.org/10.1021/acs.langmuir.6b01626.
[73] S. Arima, S. Ueno, A. Ogawa, K. Sato, Scanning Microbeam Small-Angle X-ray Diffraction Study of Interfacial Heterogeneous Crystallization of Fat Crystals in Oil-in-Water Emulsion Droplets, Langmuir 25 (2009) 9777–9784, https://doi.org/10.1021/la901115x.
[74] N. Denkov, S. Tcholakova, I. Lesov, D. Cholakova, S.K. Smoukov, Self-shaping of oil droplets via the formation of intermediate rotator phases upon cooling, Nature 528 (2015) 392–395, https://doi.org/10.1038/nature16189.
[75] S. Guttman, Z. Sapir, M. Schultz, A.V. Butenko, B.M. Ocko, M. Deutsch, E. Sloutskin, How faceted liquid droplets grow tails, Proceedings of the National Academy of Sciences 113 (2016) 493–496. doi:10.1073/pnas.1515614113.
[76] J.N. Coupland, Crystallization in emulsions, Curr. Opin. Colloid Interface Sci. 7 (2002) 445–450, https://doi.org/10.1016/S1359-0294(02)00080-8.
[77] J. Giermanska, F. Thivilliers, R. Backov, V. Schmitt, N. Drelon, F. Leal-Calderon, Gelling of Oil-in-Water Emulsions Comprising Crystallized Droplets, Langmuir 23 (2007) 4792–4799, https://doi.org/10.1021/la070071c.
[78] F. Thivilliers, E. Laurichesse, H. Saadaoui, F. Leal-Calderon, V. Schmitt, Thermally Induced Gelling of Oil-in-Water Emulsions Comprising Partially Crystallized Droplets: the Impact of Interfacial Crystals, Langmuir 24 (2008) 13364–13375, https://doi.org/10.1021/la802521f.
[79] K. Golemanov, S. Tcholakova, N.D. Denkov, T. Gurkov, Selection of Surfactants for Stable Paraffin-in-Water Dispersions, undergoing Solid−Liquid transition of the Dispersed Particles, Langmuir 22 (2006) 3560–3569, https://doi.org/10.1021/la053059y.
[80] E. Fredrick, P. Walstra, K. Dewettinck, Factors governing partial coalescence in oil-in-water emulsions, Adv. Colloid Interface Sci. 153 (2010) 30–42, https://doi.org/10.1016/j.cis.2009.10.003.
[81] L.E. Low, S.P. Siva, Y.K. Ho, E.S. Chan, B.T. Tey, Recent advances of characterization techniques for the formation, physical properties and stability of Pickering emulsion, Adv. Colloid Interface Sci. 277 (2020) 102117, https://doi.org/10.1016/j.cis.2020.102117.
[82] J. Frelichowska, M.-A. Bolzinger, Y. Chevalier, Effects of solid particle content on properties of o/w Pickering emulsions, J. Colloid Interface Sci. 351 (2010) 348–356, https://doi.org/10.1016/j.jcis.2010.08.019.
[83] V. Vasile, Experimental study of the thermal and rheological behaviour of paraffin-in-water emulsions used as a secondary refrigerants, phdthesis, Université de Lyon ; Universitatea politehnica (Bucarest), 2019. https://theses.hal.science/tel-02402732 (accessed May 17, 2023).
[84] D. Rasselet, M.F. Pucci, A.-S. Caro-Bretelle, J.-M. Lopez-Cuesta, A. Taguet, Peculiar Morphologies Obtained for 80/20 PLA/PA11 Blend with Small Amounts of Fumed Silica, Nanomaterials 11 (2021) 1721, https://doi.org/10.3390/nano11071721.
[85] T. Sawaya, I. Mokbel, N. Ainous, E. Rauzy, C. Berro, J. Jose, Experimental Vapor pressures of six n-Alkanes (C21, C23, C25, C27, C29, C30) in the Temperature Range between 350 K and 460 K, J. Chem. Eng. Data 51 (2006) 854–858, https://doi.org/10.1021/je050182i.
[86] L. Hohl, S. Röhl, D. Stehl, R. von Klitzing, M. Kraume, Influence of Nanoparticles and drop size Distributions on the Rheology of w/o Pickering Emulsions, Chem. Ing. Tech. 88 (2016) 1815–1826, https://doi.org/10.1002/cite.201600063.
[87] H. Barthel, Surface interactions of dimethylsiloxy group-modified fumed silica, Colloids Surf A Physicochem Eng Asp 101 (1995) 217–226, https://doi.org/10.1016/0927-7757(95)03179-H.
[88] S.F. Velandia, P. Marchal, C. Lemaitre, V. Sadtler, T. Roques-Carmes, Evaluation of the repartition of the particles in Pickering emulsions in relation with their rheological properties, J. Colloid Interface Sci. 589 (2021) 286–297, https://doi.org/10.1016/j.jcis.2021.01.005.
[89] M. Dinkgreve, K.P. Velikov, D. Bonn, Stability of LAPONITE®-stabilized high internal phase Pickering emulsions under shear, Phys. Chem. Chem. Phys. 18 (2016) 22973–22977, https://doi.org/10.1039/c6cp03572h.
[90] H.A. Barnes, Rheology of emulsions — a review, Colloids Surf A Physicochem Eng Asp 91 (1994) 89–95, https://doi.org/10.1016/0927-7757(93)02719-U.
[91] S.R. Derkach, Rheology of emulsions, Adv. Colloid Interface Sci. 151 (2009) 1–23, https://doi.org/10.1016/j.cis.2009.07.001.
[92] L. Huang, M. Petermann, C. Doetsch, Evaluation of paraffin/water emulsion as a phase change slurry for cooling applications, Energy 34 (2009) 1145–1155, https://doi.org/10.1016/j.energy.2009.03.016.
[93] M.M. Cross, Rheology of non-Newtonian fluids: a new flow equation for pseudoplastic systems, J. Colloid Sci. 20 (1965) 417–437, https://doi.org/10.1016/0095-8522(65)90022-X.
[94] K. Kaveh, A. Malcherek, Enhancing non-newtonian fluid modeling: a novel extension of the cross flow curve model, J. Hydro Environ. Res. 56 (2024) 17–27, https://doi.org/10.1016/j.jher.2024.08.001.
[95] F. Leal-Calderon, F. Thivilliers, V. Schmitt, Structured emulsions, Curr. Opin. Colloid Interface Sci. 12 (2007) 206–212, https://doi.org/10.1016/j.cocis.2007.07.003.
[96] J.D. Ferry, Viscoelastic Properties of Polymers, John Wiley & Sons, 1980.
[97] S.B. Ross-Murphy, Rheological Methods, in: S.B. Ross-Murphy (Ed.), Physical Techniques for the Study of Food Biopolymers, Springer US, Boston, MA, 1994: pp. 343–392. doi: 10.1007/978-1-4615-2101-3_7.
[98] X. Zhao, T. Wu, T. Xing, X. Xu, G. Zhou, Rheological and physical properties of O/W protein emulsions stabilized by isoelectric solubilization/precipitation isolated protein: the underlying effects of varying protein concentrations, Food Hydrocoll. 95 (2019) 580–589, https://doi.org/10.1016/j.foodhyd.2018.03.040.
[99] S. Gschwander, S. Niedermaier, S. Gamisch, M. Kick, F. Klünder, T. Haussmann, Storage Capacity in Dependency of Supercooling and Cycle Stability of Different PCM Emulsions, Appl. Sci. 11 (2021) 3612, https://doi.org/10.3390/app11083612.
[100] Liquid-solid-solid thermal behaviour of n-C44H90 + n-C50H102 and n-C25H52 + n-C28H58 paraffinic binary mixtures, Fluid Phase Equilibria 111 (1995) 253–272. doi:10.1016/0378-3812(95)02777-C.
[101] M. Nazari Sam, A. Caggiano, C. Mankel, E. Koenders, A Comparative Study on the thermal Energy Storage Performance of Bio-based and Paraffin-based PCMs using DSC Procedures, Materials 13 (2020) 1705, https://doi.org/10.3390/ma13071705.
[102] A.S. Luyt, I. Krupa, Thermal behaviour of low and high molecular weight paraffin waxes used for designing phase change materials, Thermochim Acta 467 (2008) 117–120, https://doi.org/10.1016/j.tca.2007.11.001.
[103] X. Zhang, J. Niu, S. Zhang, J.-Y. Wu, PCM in Water Emulsions: Supercooling Reduction Effects of Nano-Additives, Viscosity Effects of Surfactants and Stability, Adv. Eng. Mater. 17 (2015) 181–188, https://doi.org/10.1002/adem.201300575.
[104] K. Yan, L. Qiu, H. Li, N. Cao, Y. Feng, Expanded graphite encapsulation of nitrates for enhanced thermal transport: Mechanism insight and component screening,

Compos. Sci. Technol. 259 (2025) 110957, https://doi.org/10.1016/j.compscitech.2024.110957.
[105] K. Yan, L. Qiu, Y. Feng, Erythritol/expanded graphite form-stable phase change materials with excellent thermophysical properties, J. Storage Mater. 68 (2023) 107667, https://doi.org/10.1016/j.est.2023.107667.
[106] Nanopore Confinement-driven Synchronous Enhancement of Thermal and Mechanical Properties of Phase Change Materials - Qiu - 2025 - Angewandte Chemie International Edition - Wiley Online Library, (n.d.). https://onlinelibrary.wiley.com/doi/10.1002/anie.202500957 (accessed March 11, 2026).
[107] K. Xu, C. Wu, Z. Chen, M. Li, L. Yang, S. Ai, S. Cui, Preparation and Characterization of Lightweight, Hydrophobic, and Insulative Melamine Foam/Fumed Silica Composites, ACS Appl. Mater. Interfaces 17 (2025) 12653–12662, https://doi.org/10.1021/acsami.4c21072.
[108] T.-W. Lian, A. Kondo, T. Kozawa, T. Ohmura, W.-H. Tuan, M. Naito, Effect of fumed silica properties on the thermal insulation performance of fibrous compact, Ceram. Int. 41 (2015) 9966–9971, https://doi.org/10.1016/j.ceramint.2015.04.076.
[109] A.I. Gómez-Merino, J.J. Jiménez-Galea, F.J. Rubio-Hernández, J.L. Arjona-Escudero, I.M. Santos-Ráez, Heat transfer and Rheological Behavior of Fumed Silica Nanofluids, Processes 8 (2020) 1535, https://doi.org/10.3390/pr8121535.
[110] M. Chereches, A. Vardaru, G. Huminic, E.I. Chereches, A.A. Minea, A. Huminic, Thermal conductivity of stabilized PEG 400 based nanofluids: an experimental approach, Int. Commun. Heat Mass Transfer 130 (2022) 105798, https://doi.org/10.1016/j.icheatmasstransfer.2021.105798.
[111] A.I. Gómez-Merino, J.J. Jiménez-Galea, M.H. Spillman-Daniele, F.J. Rubio-Hernández, Experimental assessment on rheological and thermal properties of fumed silica in PPG400 nanofluids, J. Mol. Liq. 341 (2021) 117358, https://doi.org/10.1016/j.molliq.2021.117358.
[112] A. Paul, E. Baumhögger, M.-O. Dewerth, I.H. Dindar, G. Sonnenrein, J. Vrabec, Thermal conductivity of solid paraffins and several n-docosane compounds with graphite, J. Therm. Anal. Calorim. 148 (2023) 5687–5694, https://doi.org/10.1007/s10973-023-12107-2.
[113] N. Ukrainczyk, S. Kurajica, J. Šipušić, Thermophysical Comparison of five Commercial Paraffin Waxes as Latent Heat Storage Materials, accessed March 18, 2026, Chem. Biochem. Eng. Q. 24 (2010) 129–137, https://hrcak.srce.hr/en/55015.
[114] P.S. Puri, J.M. deMan, Thermal Conductivity of Liquid-Liquid Emulsions, Canadian Institute of Food Science and Technology Journal 10 (1977) 49–52, https://doi.org/10.1016/S0315-5463(77)73436-4.
[115] L. Liu, J. Niu, J.-Y. Wu, Formulation of highly stable PCM nano-emulsions with reduced supercooling for thermal energy storage using surfactant mixtures, Sol. Energy Mater. Sol. Cells 223 (2021) 110983, https://doi.org/10.1016/j.solmat.2021.110983.
[116] X. Zhang, J. Wu, J. Niu, PCM-in-water emulsion for solar thermal applications: the effects of emulsifiers and emulsification conditions on thermal performance, stability and rheology characteristics, Sol. Energy Mater. Sol. Cells 147 (2016) 211–224, https://doi.org/10.1016/j.solmat.2015.12.022.
[117] F. Wang, X. Fang, Z. Zhang, Preparation of phase change material emulsions with good stability and little supercooling by using a mixed polymeric emulsifier for thermal energy storage, Sol. Energy Mater. Sol. Cells 176 (2018) 381–390, https://doi.org/10.1016/j.solmat.2017.10.025.